AD-A187 888 COLLABORATIVE STUDIES OF POLAR CAP IONOSPHERIC DYNAMICS 1/1
(U) MICHIGAN UNIV ANN ARBOR SPACE PHYSICS RESEARCH LAB
J W MERIWETHER ET AL 12 OCT 87 AFGL-TR-87-0012
UNCLASSIFIED F19628-83-K-0035 F/G 4/1 NL

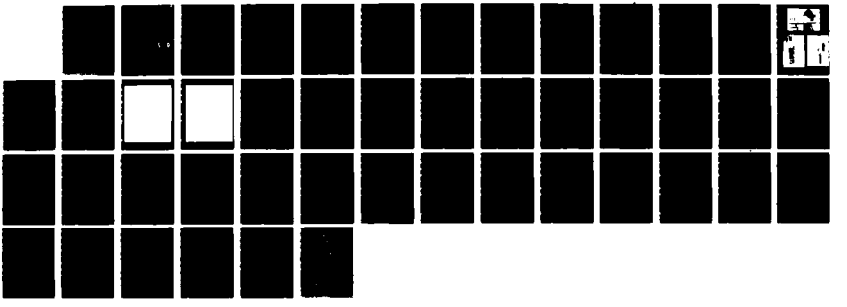

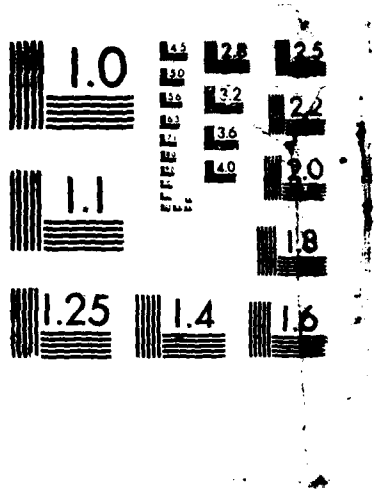

MICROCOPY RESOLUTION TEST CHART
NATIONAL BUREAU OF STANDARDS-1963-A

AFGL-TR-87-0012

(4)

AD-A187 888

Collaborative Studies of Polar Cap Ionospheric Dynamics

DTIC_FILE_COPY

J. W. Meriwether, Jr.
T. L. Killeen

University of Michigan
Space Physics Research Laboratory
Department of Atmospheric and Oceanic Sciences
Ann Arbor, Michigan 48109

12October 1987.

Final Report
Period Covered: 6/10/83 to 9/30/85

DTIC
ELECTE
DEC 04 1987
S D
H

AIR FORCE GEOPHYSICS LABORATORY
AIR FORCE SYSTEMS COMMAND
UNITED STATES AIR FORCE
HANSCOM AIR FORCE BASE, MASSACHUSETTS 01731

Approved for public release; distribution unlimited

87 11 24 098

"This technical report has been reviewed and is approved for publication"

EDWARD J. WEBER
Contract Manager
Ionospheric Effects Branch

HERBERT C. CARLSON, Chief
Ionospheric Effects Branch
Ionospheric Physics Division

FOR THE COMMANDER

ROBERT A. SKRIVANEK
Director
Ionospheric Physics Division

This report has been reviewed by the ESD Public Affairs Office (PA) and is releasable to the National Technical Information Service (NTIS).

Qualified requestors may obtain additional copies from the Defense Technical Information Center. All others should apply to the National Techncial Information Service.

If your address has changed, or if you wish to be removed from the mailing list, or if the addressee is no longer employed by your organization, please notify AFGL/DAA, Hanscom AFB, MA 01731. This will assist us in maintaining a current mailing list.

Unclassified

SECURITY CLASSIFICATION OF THIS PAGE

REPORT DOCUMENTATION PAGE

1a. REPORT SECURITY CLASSIFICATION: Unclassified	1b. RESTRICTIVE MARKINGS
2a. SECURITY CLASSIFICATION AUTHORITY	3. DISTRIBUTION/AVAILABILITY OF REPORT: Approved for public release, distribution unlimited.
2b. DECLASSIFICATION/DOWNGRADING SCHEDULE	
4. PERFORMING ORGANIZATION REPORT NUMBER(S)	5. MONITORING ORGANIZATION REPORT NUMBER(S): AFGL-TR-87-0012
6a. NAME OF PERFORMING ORGANIZATION: University of Michigan, Space Physics Research Laboratory; 6b. OFFICE SYMBOL (If applicable)	7a. NAME OF MONITORING ORGANIZATION: Air Force Geophysics Laboratory
6c. ADDRESS (City, State and ZIP Code): Ann Arbor, Michigan 48109	7b. ADDRESS (City, State and ZIP Code): Hanscom A.F.B. Massachusetts 01731
8a. NAME OF FUNDING/SPONSORING ORGANIZATION; 8b. OFFICE SYMBOL (If applicable)	9. PROCUREMENT INSTRUMENT IDENTIFICATION NUMBER: F19628-83-K-0035
8c. ADDRESS (City, State and ZIP Code)	10. SOURCE OF FUNDING NOS.

PROGRAM ELEMENT NO.	PROJECT NO.	TASK NO.	WORK UNIT NO.
61102F	2310	G9	CA

11. TITLE (Include Security Classification): Collaborative Studies of Polar Cap Ionospheric Dynamics

12. PERSONAL AUTHOR(S): J.W. Meriwether, Jr.; T.L. Killeen

13a. TYPE OF REPORT	13b. TIME COVERED	14. DATE OF REPORT (Yr., Mo., Day)	15. PAGE COUNT
Final Report	FROM 6/10/83 TO 9/30/85	10/12/87	44

16. SUPPLEMENTARY NOTATION

17 COSATI CODES			18. SUBJECT TERMS (Continue on reverse if necessary and identify by block number)
FIELD	GROUP	SUB. GR.	
			>Polar Ionosphere; Fabry-Perot Interferometer; Atmosphere Dynamics and Thermodynamics

19. ABSTRACT (Continue on reverse if necessary and identify by block number)

An important parameter in the modelling of polar cap ionospheric phenomena relating to scintillations and small scale irregularities is the thermospheric wind. The magnitude and direction of the flow of the neutral atmosphere determines how quickly these features of the polar cap morphology develop and grow. The AFGL contract (DoD-C-F19628-83-K-0035) was awarded to the University of Michigan to support the construction and installation of an automatic instrument designed to observe automatically thermospheric winds and temperatures at Thule Air Base in Greenland. The Space Physics Research Laboratory carried out this task and operated the observatory successfully throughout the 1985/1986 winter between early December 1985 and 1 April 1986. This report presents a description of the instrumentation and a set of plots showing the reduced set of observations for the clear nights in this period.

20. DISTRIBUTION/AVAILABILITY OF ABSTRACT	21. ABSTRACT SECURITY CLASSIFICATION
UNCLASSIFIED/UNLIMITED ☐ SAME AS RPT. ☐ DTIC USERS ☐	Unclassified

22a. NAME OF RESPONSIBLE INDIVIDUAL	22b. TELEPHONE NUMBER (Include Area Code)	22c. OFFICE SYMBOL
Edward Weber		AFGL/LIS

DD FORM 1473, 83 APR EDITION OF 1 JAN 73 IS OBSOLETE.

Unclassified

SECURITY CLASSIFICATION OF THIS PAGE

Introduction

The two main objectives of the AFGL grant were: 1) the construction, the installation, and operation of a Fabry-Perot/spectrophotometer observatory at Thule Air Base in Greenland; and 2) automatic measurements of thermospheric winds and temperatures in addition to the measurements of airglow/aurora intensity for the major polar cap emission features throughout the 1985/86 winter. The new observatory extends the CEDAR chain of radar and optical facilities into the polar cap region close to the geomagnetic pole. Figure 1 shows the current distribution of FPI and IS radar stations in the world.

The data base attained by the Thule measurements representing thermospheric winds (at 250 km) and temperatures extended between early December, 1985 to 1 April, 1986, with a two week gap in early February, 1986. These observations are needed to increase our understanding of the dynamic state of the polar cap ionosphere, especially for the period of solar minimum. These results are needed as part of a major global effort to observe the dynamics of the thermosphere with a network of Fabry-Perot and radar observatories.

The emission features chosen for monitoring by the 0.5 m spectrophotometer were: 5200Aå of NI, 5577A of OI, 5770A of Hg, 6300A of OI, and the hydrogen geocoronal line at 6563A. In mid-February, two lines of the OH 5-1 band at 7995A and 8100A were added to determine the variation of the band intensity and rotational temperature. The Hg line serves as a check on the cloud cover over the Thule optical observatory. Cloud conditions are also monitored using the Danish Arctic Contractor's (DAC) weather records.

This final report will present a digest of the experimental details, summarize data analysis activity, and present results from the Fabry-Perot observations reduced and plotted for the 1985-86 winter. Also included is a draft of a JGR paper discussing scientific aspects of the December and January Thule observations.

Accession For	
NTIS GRA&I	☑
DTIC TAB	☐
Unannounced	☐
Justification	
By	
Distribution/	
Availability Codes	
Dist	Avail and/or Special
A-1	

Experimental aspects of the Thule Observatory

The Fabry-Perot instrument constructed for the Thule Air Base Observatory monitors thermospheric winds and temperatures in the polar cap region at Thule through measurement of the Doppler shift of the auroral/airglow emission lines of atomic oxygen at 6300 and 5577A. Since the Doppler shift corresponding to a 100 m/sec wind is 0.002A, very small spectral shifts must be measured. A Fabry-Perot interferometer at high resolution is used to achieve this objective. The nominal spacers used are 1.116 cm in thickness, which allows for ease in the determination of the Doppler shift of the 7320A emission (the emission from the O^+ doublet) without confusion in the overlap of the two components of this doublet. For 6300A, this spectral range is equivalent to the total Doppler shift of 8.6 km/sec. Nominal observations arrive at a determination of the Doppler position with an uncertainty of about 15m/sec and for the Doppler width, an uncertainty of about 50 degrees. The Doppler stability is generally excellent with less than 25 m/sec drift per night of observations. A source emitting a bright neon line at 6306A is used to determine this Doppler reference. Upon the close of each mapping cycle featuring observations in the geographic cardinal and zenith directions, the pointing head is directed to look into the calibration chamber where the neon source is located. This ensures that the full aperture of the etalon is illuminated and provides a simulation of the sky observation but with much greater counting statistics.

Typical integration times required are several minutes for 100R of source emission at 6300A and about 45 minutes for 10R of 6300A emission. Only 25 seconds are needed for the neon calibration. The configuration of the Thule Fabry-Perot interferometer is very similar to that of the Sondrestrom Optical facility (Meriwether et al., 1983; 1984). It utilizes an image plane detector developed for space flight (Killeen et al., 1983) and the experimental data is reduced according to the technique described by Killeen and Hays (1984).

Figures 3, 4, and 5 show exterior and interior photographs of the Thule optical facility in its present location at the Thule pier. Figure 3 shows the etalon temperature controlled housing and the 3-stage thermoelectric cooler for the image plane detector.

The operational principles that govern the application of the instrument are well known and can be found in the references given above. Briefly, the etalon cavity divides the incoming wave front from the sky into multiple beams that are separated in phase by the etalon gap path difference. The concentration of these multiple beams by the objective lens at the focal plane of the lens (focal length 150cm) creates the familiar interference ring pattern that is the signature of the Fabry-Perot interferometer. The diameter of the first order

is too large for the 1.2 cm diameter of the image plane detector so two lenses are used to demagnify this image by a factor of 2.

Perhaps the outstanding feature of the Thule interferometer is the use of the image plane detector (IPD). Doppler motion in the atmosphere is detected as a change in the angular position of the order of interference placed upon the face of the detector by the optics of the instrument. The detector has 12 anode elements shaped in the form of annular rings that collect photoelectrons simultaneously from the interference pattern. This detector is constructed by ITT and is identical to the one flown on the NASA Dynamics Explorer spacecraft. Its construction features a rugged design to withstand substantial vibration. The device has both pulse counting and analogue circuitry for each of the 12 channels. There is also an overload protect circuit that introduces a back bias to the high voltage when the strip current of the tube caused by high light levels surpasses the threshold of possible damage.

The quality of the observations is closely related to the spatial resolution provided by the detector. The finesse of the current IPD in use is ~ 7. The error bars for winds and temperatures are somewhat poorer than those achieved for the spacecraft instrument due to some chemical contamination introduced by the manufacturers at the time of IPD fabrication. A second tube has been ordered that will improve this performance, but will necessitate extra care to avoid premature ageing by exposure to high light levels.

The application of presssure scanning to the 6328A emission from a Ne-He frequency-stabilized laser provides the calibration needed for the determination of the individual anode detector responses to the spectral source emission profile. The analysis software uses the Fourier transforms for each channel laser scan in the evaluation of the correlation integral (Killeen and Hays, 1983).

The operations of the interferometer are determined by Fortran data-taking software in the DEC LSI 11-23 computer. The parameters needed for datataking are stored in a setup file placed upon the Winchester hard disk area and read into the program upon activation. These parameters are quantities such as integration time, look angle directions, the count level of integration corresponding to the desired level of meassurement accuracy, and the selection of filters. This file is read in by the datataking software at the beginning of observations each evening. The determination of start and stop times for datataking is carried out by a program that computes these times for a solar depression angle of 8 degrees. The use of narrow band filters with spectral width of 3A allows us to operate at solar depression angles between 8 and 14 degrees without serious hindrance from twilight background. These computations are carried out at local noon each day and requires only a few seconds.

The particular operating system used in the computer system software, known as

TSX, permits multiple FORTRAN programs to run simultaneously during the observations. This implies that real time data analysis may be undertaken during campaign efforts. The utilization of this capability in early January 1986, revealed several problems with the observations that were cleared up at that time. The existence of this capability was also very useful for editing and program development during times of attended observations.

To guard against possible mishaps introduced by computer crashes, a watchdog timer reboots the computer CPU whenever it is not reset by the computer software within any one minute. A cable linking the CPU boot switch to the watchdog timer must be installed for automatic operations from day to day. Failure to do this leads to termination of observations at the switchover from one day to the next at local noon.

The instrumentation is housed in a Wells Fargo trailer that is well-insulated to withstand the Arctic environment of low temperatures and high winds. This trailer, 24 feet long, has two plexiglass domes (Figure 1) that are used to pass light from the Arctic sky into the optical instrumentation. A double axis mirror system is enclosed within the Fabry-Perot dome to permit the observation of any region of the sky. A calibration chamber located at -85 degrees azimuth, -180 degrees zenith angle, allows the mirror system to collect light from a neon source for the determination of a Doppler reference. The entire etalon area is illuminated in this calibration work. This mirror system is placed in a stow position for travel and does not need to be removed from its mount.

This observatory was towed to AFGL in Massachusetts, and later transferred to McGuire Air Force Base for air shipment to Thule Air Base in November 1984. Its dimensions of 98 inches high and 96 inches in width permit access to a C-141 cargo plane. Because of the length of the observatory prohobited ramp access, fork-lift trucks were used to lift the vehicle to a height that would allow direct lateral motion of the trailor into the airplane. The domes were removed and stored seperately in this shipment.

The second dome houses a 0.5 m spectrophotometer that was contributed by the Ionospheric Physics Division for the purpose of determining spectral intensities for selected spectral emissions from the polar cap airglow spectrum. This instrument was installed in October, 1985, and interfaced with the LSI 11/23 computer for automatic operations. It is pointed to observe the zenith sky.

The spectral range of the spectrophotometer in normal operations is about 3100A with a spectral width of about 8A at 5200A and 5A at 8000A. The stepping drive is programmable so that any spectral emission may be selected out of this spectral range for sampling. The grating position is monitored by a shaft encoder and this value is recorded by the computer through a 16 bit BCD interface. The datataking software modifications

incorporated the spectrophotometer module used at other Michigan optical facilities to program the spectral scan of this instrument. A setup file read in the computer memory upon program activiation specifies the selection of the spectral emissions to be included within a spectral scan, the number of positions for each spectral sub-scan, and the integration period for each position.

The sky was sufficiently clear over Thule during the period of observations to enable useful measurements to be made on approximately 40% of the possible nights. Cloud cover was obtained from weather bureau records located at the base.

The observations were reduced using laser calibrations obtained in early December, 1985, and in late January and late March, 1986. Little change in the calibration finesse for the several calibrations was found, indicating that the etalon remained properly aligned throughout the four month series of observations.

The observations were reduced with two different software packages,. The Sondrestrom data analysis software was modified to analyze the Thule Fabry-Perot results. The Dynamics Explorer software was similarly modified for Thule. Comparison of the results with the two software packages found that excellent agreement was attained for the determination of Doppler shifts and temperatures.

Results

The results of the Fabry-Perot analysis for the set of clear nights in the 1985-86 season are presented here and in the appendix. Figures 5 and 6 show example results from a single 24-hour period of observations, day 292, 1985. Figure 5 shows the Doppler wind, temperature and intensity of the 6300A emission line as a function of Universal Time during this day for measurements made to the North and South of Thule. Figure 6 shows the same information derived from measurements made to the East and West. Statistical errors are shown. It can be seen that both the data quality and quantity are excellent using the Thule facility.

Figure 7 shows the yearly averaged thermospheric wind over Thule obtained using the entire set of observations from the 1985-86 and 1986-87 seasons. These winds are plotted in polar dial form (latitude and local time). Also shown for comparison in the bottom panel are the calculations of the NCAR thermospheric general circulation model made for solar minimum conditions. As can be seen there is reasonably good agreement between the Thule results and the theoretical modeling results, with both showing a generally anti-sunward neutral flow across the polar cap. Significant natural variability is seen to occur in the measurements, both in the averages and the data from individual nights (see appendix), indicating very interesting geophysical dynamical phenomena over Thule.

Summary

A computer-controlled, automatic Fabry-Perot observatory has been installed at Thule Air Base and operated successfully for the 1985-86 winter season. The instrument itself, an associated spectrophotometer, and the computer system and interfaces are all housed in a 24 foot trailor. The trailor is parked near the pier at Thule. Thermospheric winds, temperatures and emission rates have been determined routinely, leading to the first description of the polar cap thermospehre dynamics at solar minimum.

References

Killeen, T. L., and P. B. Hays, Doppler line profile analysis for a multi-channel Fabry-Perot interferometer, *Appl. Opt.*, **23**, 612-620, 1984.

Killeen, T. L., B. C. Kennedy, P. B. Hays, D. A. Symanow, and D. H. Ceckowski, Image plane detector for the Dynamics Explorer Fabry-Perot interferometer, *Appl. Optics*, **22**, 3503-3513, 1983.

Meriwether, J. W. Jr., C. A. Tepley, S. A. Price, and P. B. Hays, Remote ground-based observations of terrestrial airglow emissions and thermospheric dynamics at Calgary, Alberta, Canada, *Opt. Eng.*, **22**, 128-131, 1983.

Meriwether, J. W., Jr., P. Shih, T. L. Killeen, V. B. Wickwar, and R. G. Roble, Nighttime thermospheric winds over Sondre Stromfjord, Greenland, *Geophys. Res. Lett.*, **11**, 931-934, 1984.

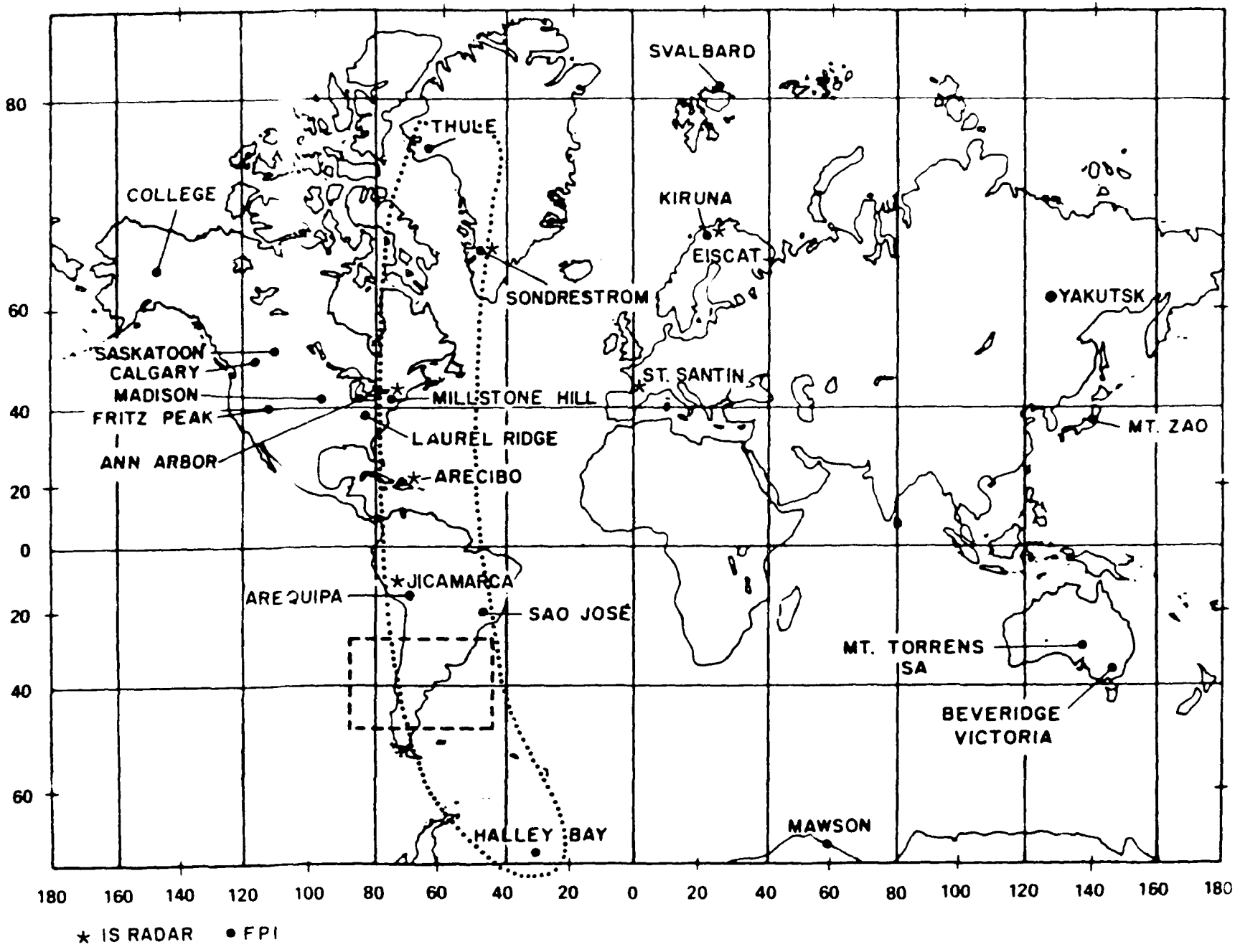
SVALBARD
THULE
COLLEGE
KIRUNA
EISCAT
SONDRESTROM
YAKUTSK
SASKATOON
CALGARY
MADISON
FRITZ PEAK
ANN ARBOR
MILLSTONE HILL
ST. SANTIN
LAUREL RIDGE
MT. ZAO
ARECIBO
JICAMARCA
AREQUIPA
SAO JOSÉ
MT. TORRENS
SA
BEVERIDGE
VICTORIA
HALLEY BAY
MAWSON
80
60
40
20
0
20
40
60
180 160 140 120 100 80 60 40 20 0 20 40 60 80 100 120 140 160 180
★ IS RADAR ● FPI

Fig. 1

Fig. 3

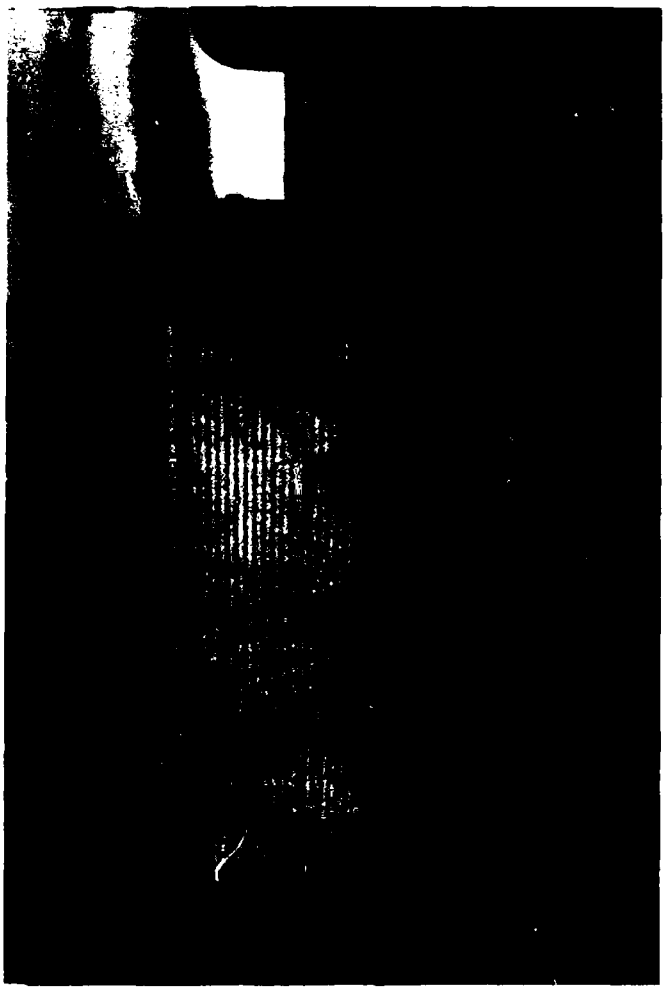

Fig. 4

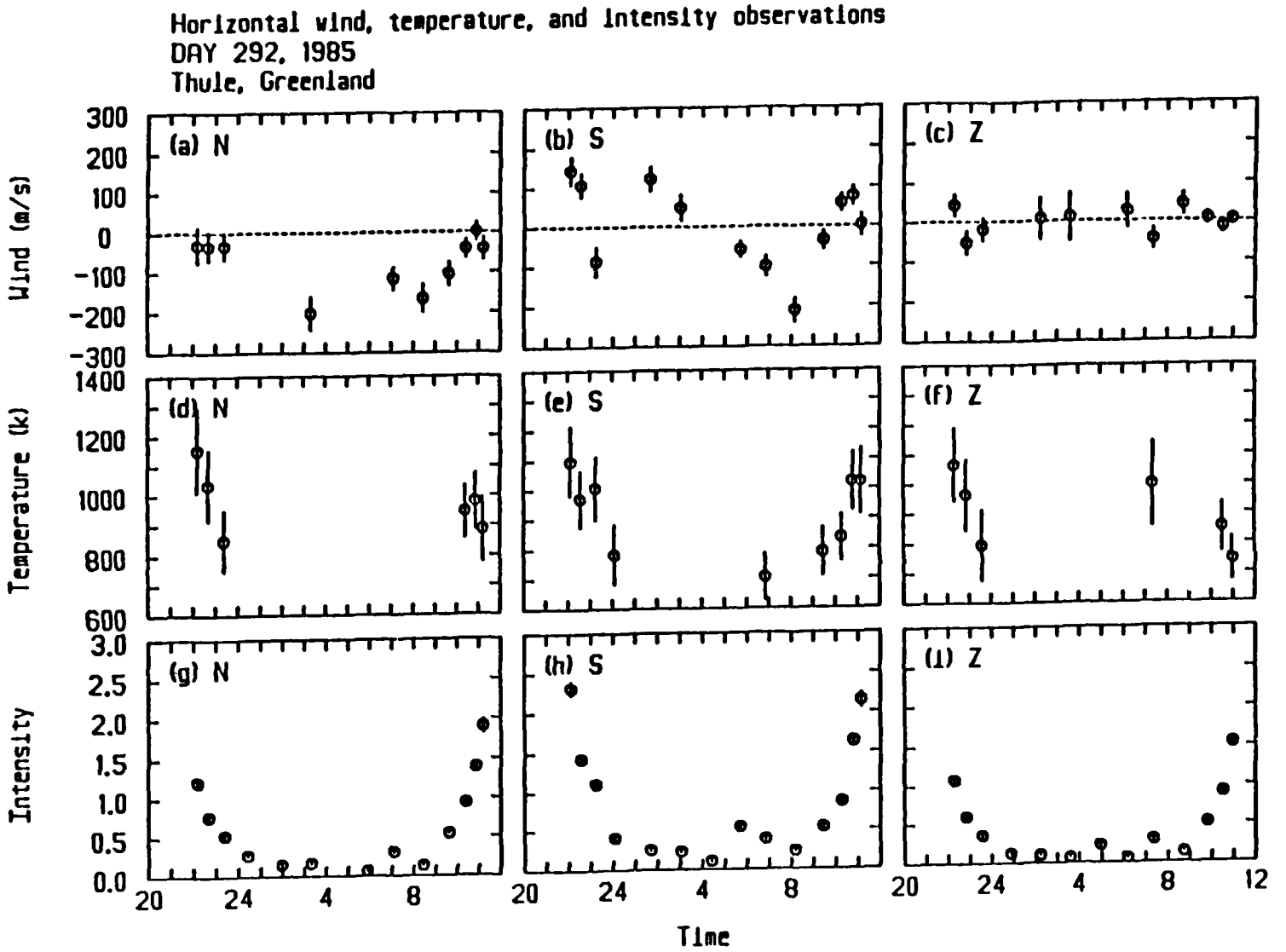
Horizontal wind, temperature, and intensity observations
DAY 292, 1985
Thule, Greenland
Wind (m/s)
Temperature (k)
Intensity
(a) N
(b) S
(c) Z
(d) N
(e) S
(f) Z
(g) N
(h) S
(i) Z
300
200
100
0
-100
-200
-300
1400
1200
1000
800
600
3.0
2.5
2.0
1.5
1.0
0.5
0.0
20
24
4
8
12
Time
NOV 18, 1985

Fig. 5

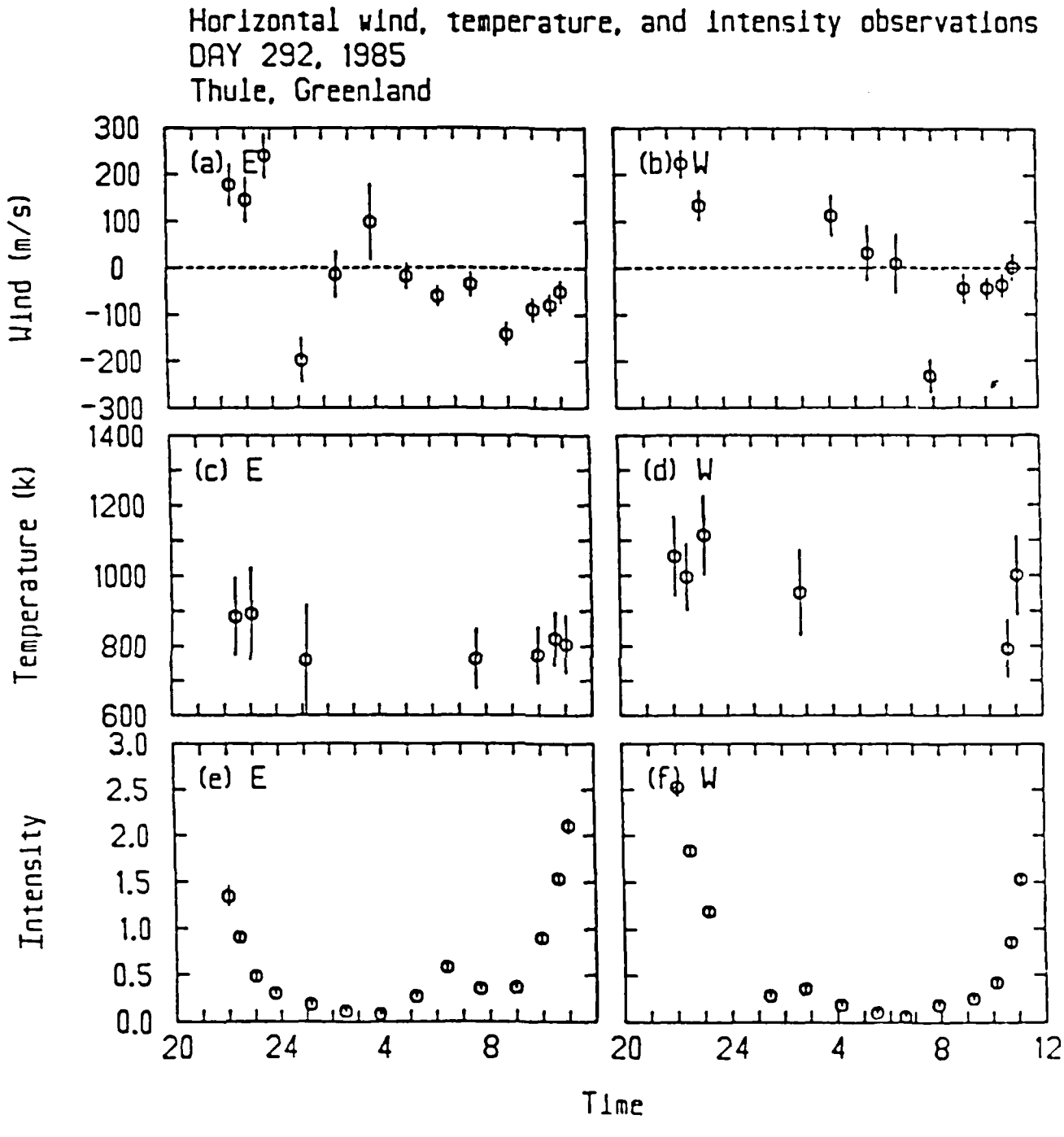
Horizontal wind, temperature, and intensity observations
DAY 292, 1985
Thule, Greenland
Wind (m/s)
300
200
100
0
-100
-200
-300
(a) E
(b) W
Temperature (k)
1400
1200
1000
800
600
(c) E
(d) W
Intensity
3.0
2.5
2.0
1.5
1.0
0.5
0.0
(e) E
(f) W
20
24
4
8
12
Time
NOV 18, 1985

Fig. 6

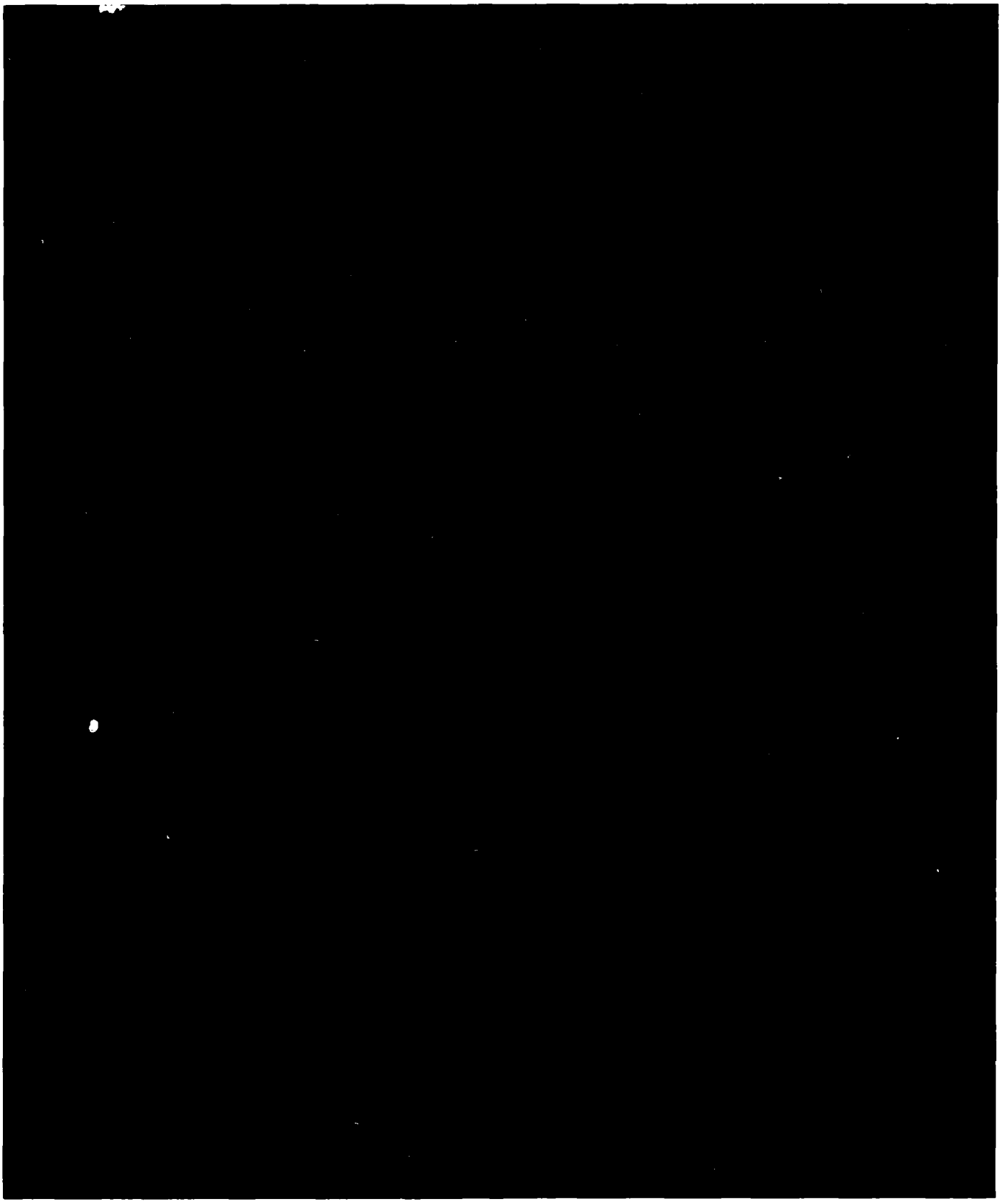

Fig. 7

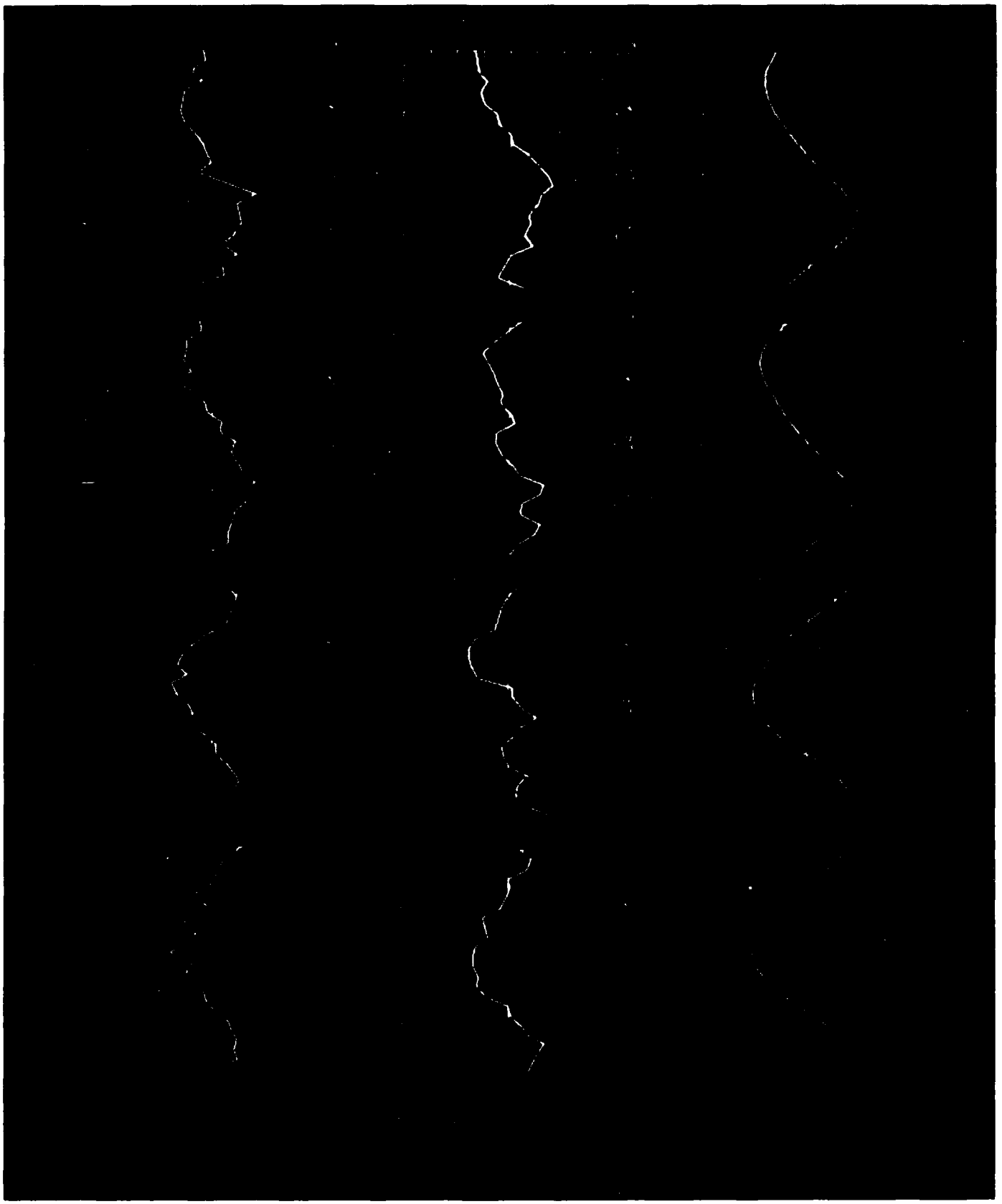

APPENDIX - SCIENTIFIC PAPER

"THERMOSPHERIC WINDS IN THE GEOMAGNETIC POLAR CAP FOR SOLAR MINIMUM CONDITIONS"

by
J. W. MERIWETHER, JR

T. L. KILLEEN

F.G. MCCORMAC

A.G. BURNS

Space Physics Research Laboratory
The University of Michigan
Ann Arbor, Michigan 48109

and

R. G. ROBLE

High Altitude Observatory
National Center for Atmospheric Research*
Boulder, CO 80307

For submission to Journal of Geophysical Research
October 1987

* The National Center for Atmospheric Research is sponsored by the National Science Foundation.

ABSTRACT

A Fabry-Perot interferometer located at Thule, Greenland (L=86) has monitored the F-region thermospheric neutral wind over the northern hemisphere geomagnetic polar cap during the 1985/86 solar minimum, winter solstice period. The wind observations were obtained by determining the Doppler shift of the (OI) 15,867 K (630.0 nm) emission. The instrument was in an automatic, 24 hours-a-day, data-collection mode during this polar-night period and the coverage was limited only by occasional clouds at the observing site. We present a subset of the measurements made during December 1985 - January 1986. Three factors make this data-set unique and particularly valuable for a study of the effects of the deposition of energy and momentum from the magnetosphere into the high-latitude neutral thermosphere. These factors are: 1) the proximity of the observing station to the geomagnetic pole, 2) the continuous nature of the coverage due to the high geographic latitude and polar night conditions, and 3), the fact that the data set was obtained near solar-minimum. The measured winds are compared with the simulations of the NCAR-thermospheric general circulation model (TGCM). The results show that winds in the geomagnetic polar cap have a fundamental diurnal character, in accord with model predictions, with typical speeds of ~200m/sec, generally in an anti-sunward direction. A large degree of variability, however, in both the magnitude and direction of the winds is observed, including evidence for curvature in the neutral flow within the region of observation (~400km diameter) of the instrument. Acceleration of the meridional component across Thule is observed at times. This acceleration is ascribed to regions of ion-drag forcing associated with the magnetospheric input of energy and momentum. Characteristic asymmetric wind signatures were seen that were well correlated with positive or negative changes in the B_y component of the interplanetary magnetic field.

INTRODUCTION

During the last few years the dynamics of the high-latitude thermosphere have received considerable experimental and theoretical attention [Killeen, 1987]. Results from the Dynamics Explorer (DE-2) satellite [e.g., Killeen, et al., 1982, 1983a, 1984a,b, 1985, 1986a; Mayr et al., 1985; McCormac et al., 1985; Hays et al., 1984] were obtained during the 1981-1983 solar-maximum period and have been compared with detailed theoretical predictions from thermospheric general circulation models (TGCMs) [e.g., Rees et al., 1983, 1985a, 1986; Hays et al., 1984; Roble et al., 1983, 1984; Killeen et al., 1986a]. The comparisons have led to the revision of the model formulations and, therefore, have improved our understanding of the physical processes responsible for driving the thermospheric circulation. Measurements made by ground-based Fabry-Perot interferometers located at various auroral or near-auroral latitudes [Meriwether et al., 1984; Sica et al., 1986; Rees et al., 1980; Smith, 1980; Smith et al., 1985; Killeen et al., 1986a] have also been interpreted using predictions from the theoretical models. Additional wind information has been derived from rocket experiments [e.g., Rees, 1971; Meriwether et al., 1973; Heppner and Miller, 1982; Rees et al., 1980] and incoherent scatter radars [Wickwar, 1984; Wickwar et al., 1984]. A review of the published literature reveals that by far the majority of the experimental data and theoretical studies reported to date pertain to solar-maximum conditions. In particular, no experimental results have yet been reported that describe the dynamics of the thermosphere within the geomagnetic polar cap for solar minimum conditions.

There are several reasons why such measurements would be of particular theoretical interest. The extensive satellite database from DE-2 was restricted to solar maximum conditions and, consequently, the theoretical models have been extensively tested and refined for those conditions. It would be of great interest to determine whether the improved models are also able to predict solar-minimum dynamical structure satisfactorily or whether further modifications are required. Instruments on DE-2 commonly observed high-speed winds (up to ~800m/s) in the polar cap. Whereas such rapid motions are in accord with current TGCM predictions for solar-maximum, magnetically-active conditions, the models generate lower wind speeds for solar minimum. These latter predictions require experimental verification.

The geomagnetic polar cap is an ideal location for studies of the energy and momentum coupling between the thermosphere and magnetosphere through measurement of neutral winds. This is because the winds driven by ion-drag forces of magnetospheric origin are, in

essence, "superimposed" upon the trans-polar winds driven by solar UV and EUV heating [Roble et al., 1982; Killeen et al., 1983a]. The "separability" of magnetospherically-driven and solar-driven winds is a consequence of the largely divergence-free nature of the former and the largely irrotational nature of the latter [Rishbeth and Hanson, 1974; Volland, 1979]. Studying the properties of these two driving functions from the database of observed winds and temperatures is a task made easier for a station capable of attaining continual day-to-day observations.

DE-2 and ground-based studies [Killeen et al., 1985; McCormac et al., 1985; Rees et al., 1986; Meriwether and Shih, 1987] have shown that the thermospheric wind structure at high latitudes often bears characteristic signatures that can be related to the magnitude and orientation of the interplanetary magnetic field (IMF). Calculations on the strength of the coupling between the motions of the ionosphere and the neutral atmosphere by Ponthieu et al.[1987] have demonstrated the response of the thermosphere to the ion drag driving function will vary substantially between solar maximum and solar minimum as a consequence of the lower levels of electron density and ionospheric conductivities existing for solar minimum. The increase in the time constant for momentum transfer from ions to neutrals during solar minimum implies that the neutral atmosphere winds will not respond readily to the fine structure of the plasma motion in the polar cap and consequently, the IMF B_y/B_z signatures should be less pronounced.

Geomagnetic-polar-cap thermospheric winds are simpler to interpret than similar measurements made from within or near the auroral zone in terms of magnetospheric storm and substorms effects. The interpretation of measurements made from locations near spatial boundaries in the aurora and/or ionospheric convection pattern often suffers from the ambiguity that arises between effects on the local winds due to significant temporal changes in the nature of the wind pattern or due to relatively small motions in the location of the spatial boundaries of a quasi-stable pattern. Since the boundaries move poleward and equatorward in response to changes in magnetic activity, auroral oval stations sample different regions of circulation and geomagnetic effects are difficult to discern [Wickwar et al., 1984; Sica et al., 1986]. At Thule, no 'boundaries' exist and geomagnetic effects are easier to deduce.

In this paper we present thermospheric observations obtained during the polar-night months of December, 1985, and January, 1986, by the AFGL/University of Michigan FPI observatory located at the Thule Air Base in Greenland. This location (L=86) lies well within the geomagetic polar cap. The stations of next-highest geomagnetic latitude are Svalbard (Norway, L=75), and Sondrestrom (Greenland, L=74), which have been used extensively for polar cusp [Smith, 1980; Smith and Sweeny, 1980; Smith et al., 1985; McCormac and

Smith, 1984] and polar cap/auroral oval boundary measurements [Meriwether et al., 1984; Herrero et al., 1984, Meriwether, 1987], respectively.

In this paper we present data selected from the 1985/1986 winter solstice period to illustrate the basic character of the solar-minimum geomagnetic polar cap wind. The comparison with predictions from the solar maximum and solar minimum NCAR-TGCMS is discussed and the results of this first study using the AFGL/UM facility are then summarized. These comparisons show that during geomagnetic quiet times the discrepancies between the TGCM modelling for solar minimum conditions and the observations are not large. However, observations during geomagnetically active periods show indications of asymmetry in the neutral wind pattern with intensifications, or "jets" of the neutral wind field that are found either in the morning or evening sectors. Examination of the IMF parameters for the two data sets chosen for this study revealed the expected correlation in which the morning "jet" corresponds to positive B_y and the evening "jet" to negative B_y. This correlation implies that ion drag forcing of the neutral gas remains significant even for solar minimum conditions.

MEASUREMENTS

The automated, Fabry-Perot interferometer system at Thule is similar to those operated in Calgary (Alberta), Sondrestrom (Greenland), and Arequipa (Peru) [Meriwether et al., 1983; Meriwether et al., 1984; Meriwether, 1987; Meriwether et al., 1986]. The Thule system is housed in a 24 ft transportable trailer located at the pier of the Thule harbor facility. The interferometer uses a segmented anode image plane detector [Killeen et al., 1983b], and a 10 cm diameter etalon to measure emission line profiles of the thermospheric (OI) 15,867 K (630 nm) airglow or auroral emission. The set of 12 detector channels spans a field of view about 0.3 degree in extent, which is about half the free spectral range. The pressure in the etalon chamber is set to place the peak of the 630.0nm source emission profile as a ring near the central portion of the field of view. The background continuum is measured with the active elements in the outer portion of the field of view. The sensitivity of the instrument at the peak of the emission line is 0.05 counts/s/Rayleigh, a value that has been confirmed by independent measurements of emission line brightness using a 1 meter Ebert/Fastie spectrometer.

The etalon plates are optically contacted with posts of 1.116 cm thickness, and the consequence of this combined with the application of the image plane detector is a stable system that exhibits diurnal variation of the Doppler reference of less than 30 m/s. The selection of the etalon gap was chosen in part to allow the complete separation of the components of the 732.0nm O^+ doublet [Meriwether et al., 1974]; while solar minimum conditions currently prohibit the use of 732.0nm emissions to detect Doppler shifts of the moving plasma [Smith et al., 1982], we anticipate that these measurements will be more feasible during the upcoming solar maximum period in 1988-1992.

Fringes are obtained sequentially at zenith angles of 45 degrees in the four cardinal directions as well as the zenith. The sky measurements are interspersed with dark count and neon gas-discharge lamp spectral calibration measurements. The time taken for a full sky cycle yielding winds of accuracies ~20-25 m/s in all directions, and including the calibrations, is determined by the brightness of the OI emission; typical values during the polar night vary between ~7 minutes at local noon to ~200 minutes near midnight for source brightnesses ranging between 100R and 5R, respectively.

The wind values are derived from the measured line-profiles using the analysis method of Killeen and Hays (1984), assuming that no appreciable vertical component occurs at the sampled volumes, and that the zero wind position is given by the ensemble average of the zenith measurements. The instrument function was measured periodically using a frequency-

stabilized laser and deconvolved numerically from measured line profiles to provide the geophysical observables: wind, temperature, emission brightness, and continuum background brightness.

RESULTS and DISCUSSION

OBSERVATIONS

Wind measurements were made during December, 1985, and January, 1986, with 24 hour daily coverage except when cloudy at Thule. The entire dataset extended to 1 April, 1986. Figure 1 summarizes the solar flux and the magnetic activity variations for this winter period. The 10.7 cm solar flux varied between 67 and 83, and the A_p index between 3 for quiet conditions and 54 for the most active period.

Figure 2 presents the variation of the hourly-averaged interplanetary magnetic parameters, B_X, B_Y, and B_Z, for two periods within this span. These data are needed for the evaluation of the relationship of the observed neutral wind field with the direction of the interplanetary magnetic field, but unfortunately, IMF measurements were not available for the entire period. In both data sets chosen there is seen a systematic variation of B_Y from positive to negative. The B_Z component, in December for the period chosen, days 352-360, turned northwards on day 352 reaching a positive level of about 10 nanotesla, and returned to the zero level by day 355.

A 5 day uninterrupted sequence of horizontal winds derived from observations in the four cardinal geographic positions is shown in Figure 3. These measurements were made between local mean noon, 16 UT, 16 December, to local mean noon, 16 UT, on the 21 December, 1985. (Local solar noon occurs at about 16.6 UT). Figure 4 presents a similar set of wind observations for four continuous days in mid-January. K_p values are indicated in each figure.

Included in both figures are theoretical calculations of the neutral wind field for quiet conditions (cross tail potential of 20 KV) derived from the NCAR thermospheric general circulation model for solar minimum and solar maximum conditions. These curves show the predicted diurnal variation at Thule at the geopotential height of ~250 km using two diurnally-reproducible runs of the NCAR TGCM. This height is taken to represent the centroid height of the volume emission profile appropriate for Thule observations of airglow and polar cap auroral emissions. Both runs were for winter solstice conditions.

The small difference in the phase of the wind diurnal variation between the two theoretical curves corresponding to solar maximum and solar minimum is caused by the

decrease in the pressure level corresponding to the smaller exospheric temperature at solar minimum. We note also that the amplitudes of the model zonal and meridional components for solar minimum are reduced by about 10% from the speeds shown for solar maximum conditions.

To aid in the interpretation of our wind measurements we show, in Figure 5, the basic wind pattern over Greenland predicted by the diurnally-reproducible TGCM model run at twelve UTs with a cross-tail potential of 20 KV. The location of the solar terminator and the approximate location of the polar cusp are also indicated in the figure. It can be seen that the theoretical predictions for the solar maximum conditions are for a polar cap wind that is anti-sunward at all UTs, with very little curvature in the direction of flow expected within the radius of observations of the Thule instrument, about 400 km at a zenith angle of 45 degrees. Also shown, in Figure 6, are model calculations of the diurnal momentum forcing terms obtained using the Diagnostic Processor of Killeen and Roble [1984]. The diurnal evolution of these forces illustrates the diurnally-reproducible balance of forces on the thermospheric gas. It can be seen that the primary polar cap forces are the ion-drag and the pressure gradient force, with the Coriolis force being also of significance. Of these forces, that due to ion drag is the most intrinsically variable.

The measurements shown in Figures 3 and 4 indicate a variation that has the basic expected diurnal sinusoidal oscillation, but also contains large departures. However, the peak amplitude of 200 m/s agreed generally well with the peak amplitude of the solar minimum model for corresponding zonal and meridional directions.

The January, 1986, observations were obtained during a period of very quiet magnetic activity. Nevertheless, the measurements show that the smooth regular diurnal variation predicted by the TGCM calculations is supplemented by higher order variations of the direction and magnitude of the thermospheric wind that differ from the fundamental made by 25-50 m/s. Larger deviations are evident at times. We note the example of 16 January where an acceleration in the anti-sunward direction is clear even when Kp values were as low as 1 or 2 during the local noon hours. There is also evident occasional lack of detailed correspondence between observations in direction pairs (North and South, East and West) at certain times. For example, the meridional observations for the midnight sector on the 18th of December (day 352) show an acceleration of the flow towards the south of about 200 m/s. Another example is the period of the 20th of December (day 354) in the nighttime sector between 01 and 08 UT, an acceleration in this instance between 0.07 and 0.1 m/s^2. As shown by the model simulation, uniform flow would require that these signatures be identical, with a small phase shift between the zonal pair of observations.

These results indicate that the thermosphere over Thule is a region where strong

magnetospheric (ion drag) forcing occurs, capable of turning the wind vector appreciably over relatively short distances. We ascribe this effect to variations in the ion drag force due, in turn, to the variability in the ion convection vector in the polar cap. Fluctuations in the ionospheric electric field have often been observed by suitably instrumented polar-orbiting satellites [Heppner, 1977].

ASYMMETRIES IN THE POLAR CAP NEUTRAL WIND PATTERN

The interesting points of the Thule FPI observations may be appreciated more readily when the observations are replotted in a polar format as shown in Figures 7 and 8. Here, orthogonal pairs of measured wind components are used to form horizontal vectors, i.e., data for the N direction combined with data for the E direction and similarly, S with W. We recognize that this procedure entails the necessary, but sometimes questionable assumption that the gradient in the wind system over the distance separating the two paired vector component observations (Tepley et al., 1984) will be insignificant. It does, however, provide a more intuitively-satisfying depiction of the polar cap flow. Once again the vector winds are compared with the predictions of the NCAR-TGCM for reference for solar cycle minimum conditions, which is included in Figure 7f and Figures 8e and 8f.

As can be seen, the predicted progression of the wind vector is a smooth rotation in the clockwise sense as the wind vector rotates with the sun, once per day. The measured vector wind shows the same progression in general, with significant departures, at times, from the sense and speed of rotation of the predicted behavior.

Perhaps the most striking feature of Figure 7 in the December 1985 polar dial plots is the asymmetry of the neutral wind field in which stronger winds were seen in the morning period between local midnight and 06 LT for days 351 and 352 and in the evening sector for days 353 and 354. Figure 2 shows increases in the magnitudes of B_y and B_z from negative levels to positive levels accompanying the increase in magnetic activity to a level in K_p of 6-. The adjustment in the asymmetry of the polar cap thermospheric winds during this transition of the magnitude and sign of B_y indicates the strong control of the polar cap neutral winds exerted by the plasma convection forcing.

Similar regions of enhanced speeds of the thermospheric neutral wind may be found in Figure 8 for days 17 and 18 in January, 1986, when the magnetic activity again increased significantly. The neutral wind pattern looks relatively symmetric for days 15 and 16, for which B_y values were near zero or slightly positive. This pattern becomes asymmetric on days 17 and 18 with faster winds seen in the evening sector between 14 and 20 hours local

time. Here, in this case, Figure 2 shows the B_y IMF parameter for days 17 and 18 had decreased to negative values. It seems evident, again, that these regions of intensification of the neutral wind field are caused by the B_y-dependent plasma convection pattern over Thule resulting from the coupling of the Earth's planetary depole field with the Sun's interplanetary magnetic field.

In several cases an acceleration in the midnight sector in the anti-sunward direction can be seen in the observations. Days 351, 352, 353,354, and 16 may be cited as examples. This result is in agreement with the predictions of the TGCM model which in Figure 5 show acceleration in the thermosphere over Thule for the UT periods 01, 03, 05, and 07 which represent the midnight sector at Thule.

There is also considerable evidence of the turning of the southern vector as compared with the northern neutral wind vector indicating the strong degree of control by local ion forcing in the Thule ionosphere. This behavior is evident in the midnight sector for days 351, 352, 16, and 17 . The same response may be seen in the plot of Greenland thermospheric winds in Figure 5 for the midnight hours, but not as clearly as shown in the observations. The TGCM computations displayed in Figure 5 were carried out for quiet magnetic conditions and the ion forcing component needed to simulate the observations properly would be considerably stronger.

REDUCED NEUTRAL FLOW DURING MAGNETIC DISTURBANCES

An interesting example of the response of the central polar cap winds to an increase in magnetic activity is the period 16-24 UT on the 18th of December (day 352). As discussed previously, the K_p index increased from 2^- to 6^- during this time; the activity remained high throughout the 19th (day 353) at about $K_p = 4$. The B_z observations depicted in Figure 2 show that this was a period of a northward turning of the z-component of the interplanetary magnetic field. We note the rather large discrepancies between the model TGCM curves and the observations during the local noon periods for the 18 and 19, December, 1985. The observations show the meridional wind to be virtually zero on the 18th at 16 UT whereas the TGCM calculations reflecting the solar driven component of the driving forces predicts a meridional flow poleward of about 200 m/s. Also notable is the observed decrease in the zonal component of the wind to speeds of a few tens of m/s during this period preceded by the several large zonal wind fluctuations in the period between 12 and 16 UT. The subsequent increase of K_p to 6^-, however, did result in increased rate of flow by a factor of 2 beyond the model curves for the two zonal components.

Another example of this reduction of the central polar cap flow during enhanced magnetic conditions is shown in the observations displayed in Figure 9 obtained on 29/30 December, 1985, (day 363), for which Figure 1 shows the Ap index was enhanced to a level of 40. In this case the meridional observations for the noon sector show that the winds in both directions are markedly reduced below the solar minimum level. The zonal motion normally eastward between 20 and 02 UT is actually reversed in the eastward set of observations and reduced for the westward direction. Data for B_y and B_z parameters available only for day 364 between 0 and 12 UT showed B_y positive and B_z negative except for a brief period at 04-06 UT, when the B_z value increased to about zero.

The fact that the amplitude of both meridional and zonal components was so small, i.e., nearly zero, under conditions of moderately active magnetic disturbances is surprising. Normally, increases in magnetic activity result in enhanced anti-sunward polar plasma convection with higher speeds of the neutral atmosphere caused by the resultant ion drag forcing. Observations by Smith et al.[1984] for Spitsbergen have displayed the same effect: when the magnetic activity increases, the speed of the wind vector decreases to about 100 m/s, and the wind direction shifts from nearly zonal to poleward. These results were interpreted by Smith et al.[1984] to imply a relocation of the cusp equatorsward with an implication of the local heating acting to block anti-sunward flow across the polar cap.

The Thule observations suggest an alternative explanation. The asymmetry of the neutral wind pattern known to occur for IMF conditions favoring large positive or negative B_y values will cause a shift of the polar cap neutral jet away from the central polar cap region. This would place the site of Thule Air Base in a region of weakly anti-sunward flow. Examination of the DE passes shown by McCormac et al.[1985] shows cases of regions within the central polar cap adjacent to the polar jet where the speed of the F-region neutral wind is weak(<100 m/s) while the speed of the polar jet itself is of the order of 400-500 m/s.

The IMF data depicted in Figure 2 for the December observations show that the B_y index changed from negative values of -5 nanotesla to positive values between 3 and 9 nanotesla during the period of reduced winds on days 352 and 353. The neutral wind plots for days 352 and 353 portray asymmetric patterns of the opposite signs for the two nights with the jet signature found in the morning sector for day 352 and in the evening sector for day 353. The region of weak flow in the neutral wind does appear to be related to the absence of ion forcing over Thule caused by the shift of the plasma convection pattern to the morning or evening sectors. Figure 6 shows that there is little acceleration taking place over Thule during the noon hours if the ion forcing term were reduced to zero. The two remaining forces, pressure gradient and the Coriolis terms, are almost evenly balanced.

POLAR CAP INTENSITY VARIATIONS OF THE 630NM EMISSION

Examination of all sky film obtained at Qanaq, Greenland (Carlson and Weber, private communication) showed sun-aligned arc activity occurring frequently in the late December period of 1985. The period of 16 UT to 24 UT on the 18th of December (the middle portion of day 352) in Figure 2 was a good example of such a period of sun-aligned auroral activity that coincided with a northward turning of B_Z. A question of considerable interest is the extent that variations in electron densities within the polar cap will in turn be reflected in structure in the neutral wind field [Carlson et al., 1984]. The detailed correlation between arc activity and neutral wind variations as seen in these results is an important question and will be investigated further when our database of examples has been sufficiently enlarged with additional cases.

In discussing Figures 3 and 4, we pointed out the relative infrequency of data points during the period 0 - 12 UT, the period of lowest intensity for the (OI) emission. The geomagnetic and solar activity for this period as indicated by the data of Figure 1 was low and observed intensities of the 630.0nm source emission were weak. Figure 10a shows the intensity observations for December 17/18, an example of the diurnal variation of the 630.0nm source emission seen at Thule during quiet magnetic periods in winter. In contrast, Figure 10b displays the 630.0nm intensity variation for December 29/30, 1985, the most magnetically disturbed day of the month. The intensity changes seen between 04-06 UT were caused by auroral arcs that were primarily sun-aligned (Carlson and Weber, private communication).

SUMMARY

The first results from a Fabry-Perot interferometer station located near the geomagnetic pole at Thule, Greenland, have been presented to illustrate the diurnal wind variation over the geomagnetic polar cap at winter solstice for solar minimum. Two periods of measurements in December, 1985 and January, 1986 have been shown, illustrating the basic diurnal rotation of the wind vector with the Sun, as well as significant higher-order departures from the simple rotation. Plotting these results in the polar format indicates these differences probably correspond to neutral wind field asymmetries caused by geometrical changes related to the By-dependent forcing induced by the polar cap plasma convection pattern.

The results have been compared with the predictions of the TGCM models of the

thermosphere for solar maximum and solar minimum for quiet magnetic conditions. While the speed and diurnal variation of the wind vector are in general agreement with the model predictions for solar minimum conditions, the fine structure of the polar cap flow is observed to be more complex than expected from a consideration of the diurnally-reproducible model calculations. Specific effects observed include significant local accelerations ascribed to temporal and spatial changes in the ion-drag force vector in the polar cap due, in turn, to changes in the convection electric field. Periods of increased magnetic activity show a reduction of the flow anti-sunward in contrast with expectations. The close correlation of these events with the changes in the three IMF parameters implies that the ion forcing component of the momentum balance equation generates the asymmetry of the neutral wind field through the B_y and B_z dependence of the polar cap plasma convection.

The Thule observations, because of the proximity of the station to the geomagnetic pole, provide a valuable capability for the monitoring of effects on the central polar cap neutral thermosphere due to time dependent changes in magnetospheric forcing. The close relationship of the thermospheric wind to the structure of the plasma convection indicates a need for the simultaneous measurements of the plasma convection flow in addition to the thermospheric wind. This would provide the opportunity to model in detail the ion-neutral coupling in the polar cap thermosphere. In addition, the relationship of auroral arc activity to the changes in the thermospheric wind noted for periods of magnetic activity should be examined in more detail; the changes in the conductivity of the F-region ionosphere implied by polar cap auroral activity will influence the coupling of the neutral atmosphere to the ionospheric motions mapped from the magnetosphere into the polar cap region.

ACKNOWLEDGEMENTS

The work was supported by AFGL grant number F19628-86-K-0037 to the University of Michigan and by NSF grant number ATM-8419806. We thank Dr. H. C. Carlson and Dr. E. Weber, Ionospheric Physics Division, Air Force Geophysics Laboratory, for their encouragement and support in the performance of this project. We also thank Dr. J. King for the use of the IMF data from IMF J shown in this paper.

FIGURE CAPTIONS

Figure 1. Variation of the solar activity $F_{10.7}$ index and magnetic activity index A_p for the December, 1985, and January, 1986, months.

Figure 2. Variation of the three IMF parameters, B_x, B_y, B_z, for December, 1985, and January, 1986, days.

Figure 3. Thule FPI observations of line-of-sight winds in the four cardinal geographical directions for the period between 16 UT, 16 December, to 16 UT, 21 December, 1985. Also shown are TGCM-NCAR calculations for moderate magnetic activity at solar minimum (cross-tail potential, 30 keV) and solar maximum conditions.

Figure 4. Same as Figure 2 but for selected days in January, 1986.

Figure 5. Neutral wind patterns over Greenland predicted by the TGCM for the Univsersal Times indicated.

Figure 6. Magnitudes of the expected diurnal momentum forcing terms for the central polar cap region.

Figure 7. Polar vector plots for Thule FPI wind observations and the solar maximum and solar minimum TGCM NCAR calculations for the December 1985 observations.

Figure 8. Same as Figure 6, but for the January, 1986 period.

Figure 9. Thule FPI observations of thermospheric winds in the four cardinal directions for the magnetically disturbed day, 29/30 December, 1985.

Figure 10. Thule 630.0nm intensities for a quiet day, 6/7 December, 1985, and a magnetically disturbed day, 29/30 December, 1985.

REFERENCES

Carlson, H.C., Jr., V.B. Wickwar, E. J. Weber, J. Buchau, J.G. Moore, W. Whiting, Plasma characteristics of polar cap F-layer arcs, *Geophys. Res. Letts.*, **9**, 895-898, 1984

Hays, P. B., T. L. Killeen, N W. Spencer, L. E. Wharton, R. G. Roble, B. E. Emery, T. J. Fuller-Rowell, D. Rees, L. A. Frank and J. D. Craven, Observations of the dynamics of the polar thermosphere, *J. Geophys. Res*, **89**, 5597, 1984.

Herrero, F. A., H. G. Mayr, I. Harris, and F. Varosi, Thermospheric gravity waves near the source: Comparison of variations in neutral temperature and vertical velocity at Sondre Stromfjord, *Geophys. Res. Letts.*, **11**, 939-942, 1984

Heppner, J. P. and M. L. Miller, Thermospheric winds at high latitudes from chemical releases, *J. Geophys. Res.*, **87**, 1633-1647, 1982.

Killeen, T.L., Energetics and dynamics of the Earth's thermosphere, *Rev. Geophys.*, **25**, 433-454, 1987

Killeen, T. L., and P. B. Hays, Doppler line profile analysis for a multi-channel Fabry-Perot interferometer, *Appl. Opt.*, **23**, 612-620, 1984.

Killeen, T. L., and R. G. Roble, An analysis of the high-latitude thermospheric wind pattern calculated by a thermospheric general circulation model, 1, Momentum forcing, *J. Geophys. Res.*, **89**, 7509-7522, 1984.

Killeen, T. L., P. B. Hays, N. W. Spencer, L. E. Wharton, Neutral winds in the polar thermosphere as measured from Dynamics Explorer, *Geophys. Res. Lett.*, **9**, 957-960, 1982.

Killeen, T. L., P. B. Hays, N. W. Spencer, L. E. Wharton, Neutral winds in the polar thermosphere as measured from Dynamics Explorer, Adv. Space Res., **2**, 10, 133-136, Pergamon Press, Oxford, 1983a.

Killeen, T. L., B. C. Kennedy, P. B. Hays, D. A. Symanow, and D. H. Ceckowski, Image plane detector for the Dynamics Explorer Fabry-Perot interferometer, *Appl. Optics*, **22**, 3503-3513, 1983b.

Killeen, T. L., P. B. Hays, G. R. Carignan, R. A. Heelis, W. B. Hanson, N. W. Spencer, and L. H. Brace, Ion-neutral coupling in the high-latitude F-region: Evaluation of ion heating terms from Dynamics Explorer 2, *J. Geophys. Res.*, **89**, 7495-7508, 1984a

Killeen, T. L., R. W. Smith, P. B. Hays, N. W. Spencer, L. E. Wharton, and F. G. McCormac, Neutral winds in the high latitude winter F-region: Coordinated observations from ground and space, *Geophys. Res. Lett.*, **11**, 311-314, 1984b

Killeen, T. L., R. A. Heelis, P. B. Hays, N. W. Spencer, and W. B. Hanson,Neutral motions in the polar thermosphere for northward interplanetary magnetic field, *Geophys. Res., Lett.*, **12**, 159-162, 1985.

Killeen, T. L., R. G. Roble, R. W. Smith, N. W. Spencer, J. W. Meriwether, Jr., D.

Rees, G. Hernandez, P. B. Hays, L. L. Cogger, D. P. Sipler, M. A. Biondi, and C. A. Tepley, Mean neutral circulation in the winter polar F-region, *J. Geophys. Res.*, **91**, 1633-1649, 1986a

Killeen, T. L., R. G. Roble, and N.W. Spencer, A computer model of global thermospheric winds and temperatures, Adv. Space Res., 1986b

Mayr, H. G., I. Harris, F. Varosi, and F. A. Herrero, Global excitation of wave phenomena in a dissipative multiconstituent medium 2. Impulsive perturbations in the earth's thermosphere, *J. Geophys. Res.*, **89**, 10961-10986, 1984

McCormac, F. G., and R. W. Smith, The influence of the interplanetary magnetic field Y component on ion and neutral motions in the polar thermosphere, *Geophys. Res. Lett.*, **11**, 935-938, 1984.

McCormac, F. G., T. L. Killeen, E. Gombosi, P. B. Hays, and N. W. Spencer, Configuration of the high-latitude neutral thermosphere circulation for IMF By negative and positive, *Geophys. Res. Lett.*, **12**,155-158, 1985.

Meriwether, J. W., Jr., J. P. Heppner, J. D. Stolarik, and E. M. Wescott, Neutral winds above 200 km at high latitudes, *J. Geophys. Res.*, **78**, 6643-6661, 1973.

Meriwether, J. W., Jr., P. B. Hays, K. D. McWatters, and A. F. Nagy, Interferometric measurements of the 7319A doublet emissions of OII, *Planet. Space Sci.*, **22**, 636-638, 1974

Meriwether J. W. Jr., Observations of thermospheric dynamics at high latitudes from ground and space, *Radio Sci.*, **18**, 1035-1052, 1983

Meriwether, J. W. Jr., C. A. Tepley, S. A. Price, and P. B. Hays, Remote ground-based observations of terrestrial airglow emissions and thermospheric dynamics at Calgary, Alberta, Canada, *Opt. Eng.*, **22**, 128-131, 1983.

Meriwether, J. W., Jr., P. Shih, T. L. Killeen, V. B. Wickwar, and R. G. Roble, Nighttime thermospheric winds over Sondre Stromfjord, Greenland, *Geophys. Res. Lett.*, **11**, 931-934, 1984.

Meriwether, J.W., Jr., J.W. Moody, M.A. Biondi, R.G. Roble, Optical interferometric measurements of nighttime equatorial thermospheric winds at Arequipa, Peru, *J. Geophys. Res.*, **91**, 5557-5566, 1986

Meriwether, J.W., Jr., and P. Shih, On the nighttime signatures of thermospheric winds observed at Sondrestrom, Greenland, as correlated with interplanetary magnetic field parameters, Annales Geophys.,in press, 1987

Meriwether, J. W., Jr., F. G. McCormac, T. L. Killeen, Multi-instrument observations of the midnight abatement in the equatorward flow of thermospheric winds at high latitudes, to be submitted, 1987

Rees, D., Ionospheric winds in the auroral zone, J. Br. *Interplanet. Soc.*,**24**, 233, 1971.

Rees, D., T. J. Fuller-Rowell, and R. W. Smith, Measurements of high-latitude thermospheric winds by rocket and ground-based techniques and their interpretation using a three-dimensional time dependent dynamical model, *Planet. Space Sci.*, **28**, 919-932,

1980.

Rees, D., T. J. Fuller-Rowell, R. Gordon, T. L. Killeen, P. B. Hays, L. E. Wharton, and N. W. Spencer, A comparison of wind observations of the upper thermosphere from the Dynamics Explorer satellite with the predictions of a global time-dependent model, *Planet. Space Sci.*, **31**, 1299-1314, 1983.

Rees, D., R. W. Smith, P. J. Charleton, F. G. McCormac, N. Lloyd and Ake Steen, The generation of vertical thermospheric winds and gravity waves at auroral latitudes, 1. Observations of vertical winds, Planet. Space Sci., 32, 667-684, 1984a

Rees, D., M. F. Smith, and R. Gordon, The generation of vertical thermospheric winds and gravity waves at auroral latitudes--2. Theory and numerical modelling of vertical winds, Planet. Space Sci., 32, 685-705, 1984b

Rees, D., R. Gordon, T. J. Fuller-Rowell, M. Smith, G. R. Carignan,T. L. Killeen, P. B. Hays, and N. W. Spencer, The composition, structure, temperature and dynamics of the upper thermosphere in the polar regions during October to December, 1981, *Planet Space Sci.*, **33**, 617-666, 1985a

Rees, D., P. Charleton, M. Carlson, and P. Rounce, High-latitude thermospheric circulation during the Energy Budget Campaign, *Planet. Space Sci.*, **47**, 195-232, 1985b.

Rees, D., T. J. Fuller-Rowell, R. Gordon, J. P. Heppner, N. C. Maynard, N. W. Spencer, L. E. Wharton, P. B. Hays, and T. L. Killeen, A theoretical and empirical study of the response of the high-latitude thermosphere to the sense of the "Y" component of the interplanetary magnetic field, *Planet Space Sci.*, **34**, 1-40, 1986.

Rishbeth, H., and W. B. Hanson, A comment on plasma "pile-up" in the F-region, *J. Atmos. Terr. Phys.*, **36**, 703-706, 1974.

Roble, R. G., R. E. Dickinson, and E. C. Ridley, Global circulation and temperature structure of the thermosphere with high-latitude plasma convection, *J. Geophys. Res.*, **87**, 1599-1614, 1982.

Roble, R. G., R. E. Dickinson, E. C. Ridley, B. A. Emery, P. B. Hays,T. L. Killeen, and N. W. Spencer, The high-latitude circulation and temperature structure of the thermosphere near solstice, *Planet Space Sci.*, **31**, 1299-1314, 1983.

Roble, R. G., B. A. Emery, R. E. Dickinson, E. C. Ridley, T. L. Killeen, P. B. Hays, G. R. Carignan, and N. W. Spencer, The high-latitude circulation, temperature and compositional structure of the southern hemisphere polar cap during October-November, 1981,
J. Geophys. Res., **89**, 9057-9068, 1984.

Sica, R. J., M. H. Rees, G. J. Romick, G. Hernandez, and R. G. Roble, Auroral zone thermospheric dynamics, 1, Averages, *J. Geophys. Res.*, **91**, 3231-3244, 1986.

Sica, R. J., G. Hernandez, G. J. Romick, M. H. Rees, and R. G. Roble, Auroral zone thermospheric dynamics, 2, Individual Nights, *J. Geophys. Res.*, **92**, 1987

Smith, R. W., Neutral winds in the polar cap, in Exploration of the Polar Upper Atmosphere, pp 189-198. Eds. C. S. Deehr and J. A. Holtet, Reidel, 1980.

Smith, R. W. and P. J. Sweeney, Winds in the thermosphere of the northern polar cap, *Nature*, **284**, 437-438, 1980.

Smith, R. W., G. G. Sivjee, R. D. Stewart, F. G. McCormac, and C. S. Deehr, Polar cusp ion drift studies through high-resolution interferometry of O+ 7320-A emission, J. Geophys. Res., 87, 4455-4460, 1982

Smith, R. W., K. Henriksen, C. S. Deehr, D. Rees, F. G. McCormac, and G. G. Sivjee, Thermospheric winds in the cusp: dependence of the latitude of the cusp, *Planet. Space Sci.*, **33**, 305-313, 1985.

Tepley, C. A., R. G. Burnside, J. W. Meriwether, Jr., P. B. Hays, and L. L. Cogger, Spatial distribution of the thermospheric neutral wind field, Planet. Space Sci., 32, 493-501, 1984

Volland, H., Magnetospheric electric fields and currents and their influence on large-scale thermospheric circulation and composition, *J. Atmos. Terr. Phys* , **41** , 853-866, 1979.

Wickwar, V. B., Thermospheric neutral wind at -39 azimuth during the daytime sector at Sondrestrom, *Geophys. Res. Lett.*, **11** , 927-930, 1984.

Wickwar, V. B., J. W. Meriwether, Jr., P. B. Hays, and A. F. Nagy, The meridional thermospheric neutral wind measured by radar and optical techniques in the auroral region, *J. Geophys. Res.*, **89** , 10987-10998, 1984.

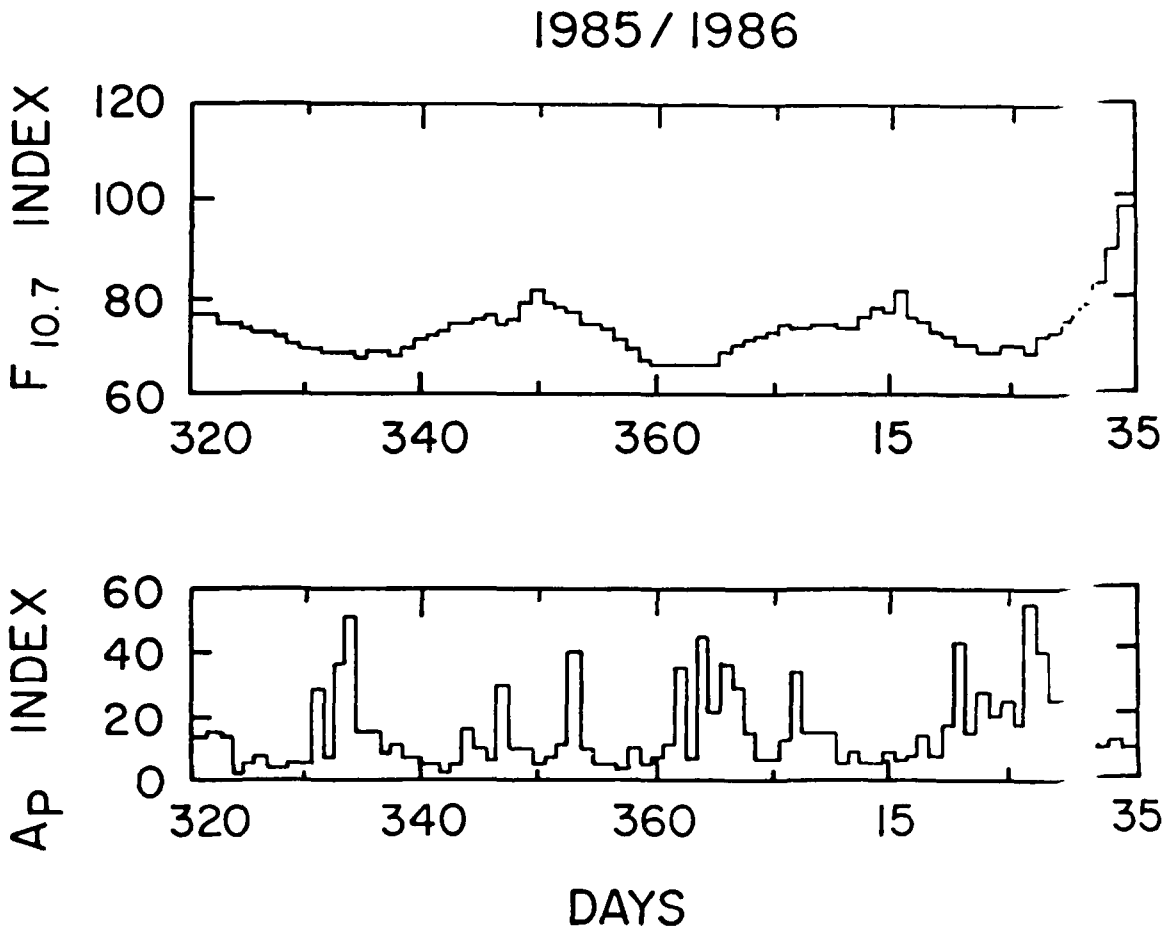
1985/1986
$F_{10.7}$ INDEX
120
100
80
60
320
340
360
15
35
Ap INDEX
60
40
20
0
320
340
360
15
35
DAYS

Fig. 1

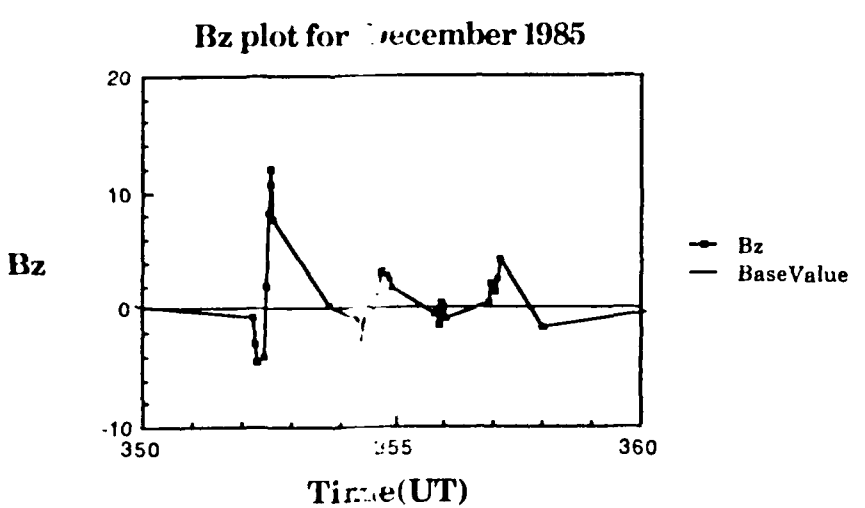
Bz plot for December 1985
Bz
Time(UT)
Bz
BaseValue

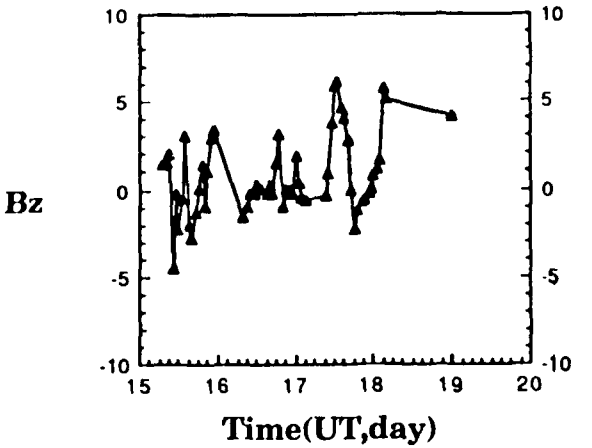
Bz
Time(UT,day)

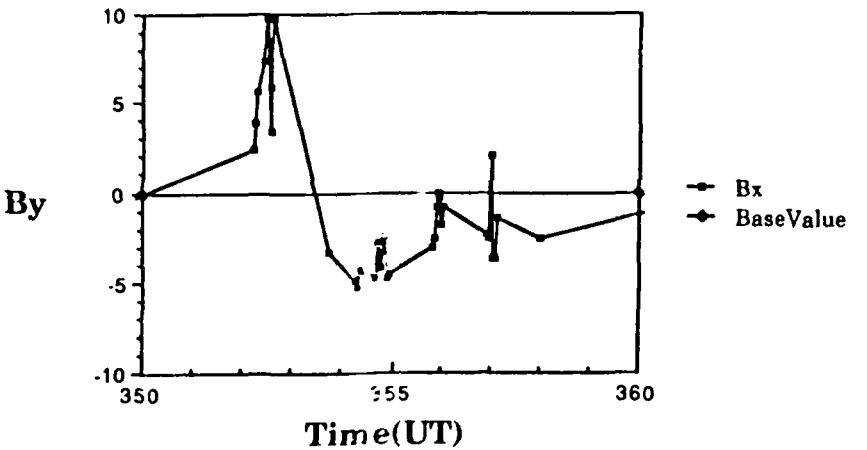
By
Time(UT)
Bx
BaseValue

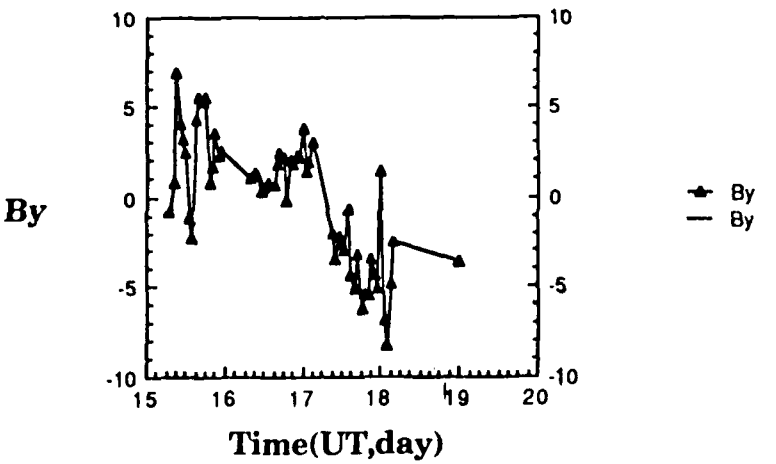
By
Time(UT,day)
By
By

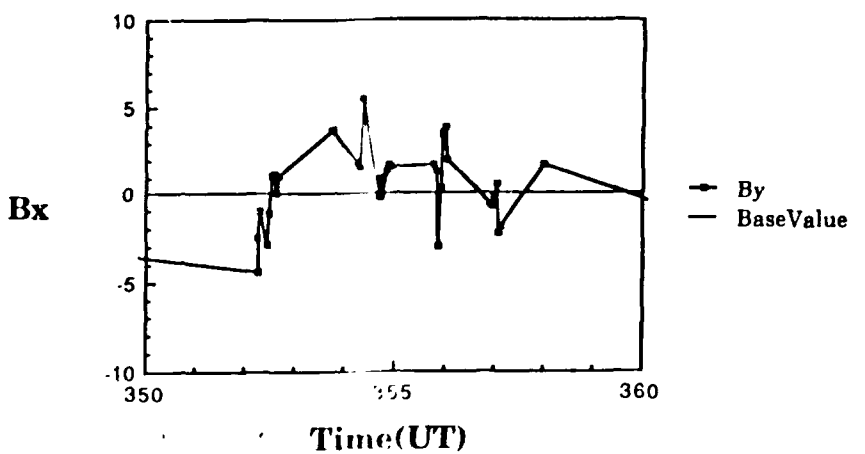
Bx
Time(UT)
By
BaseValue

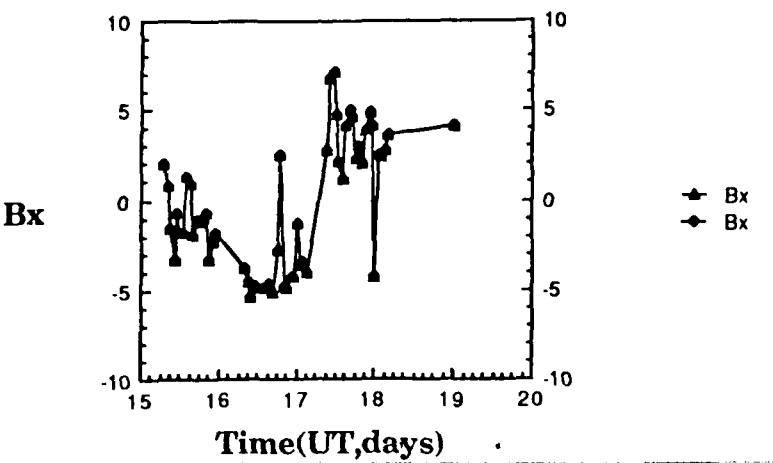
Bx
Time(UT,days)
Bx
Bx

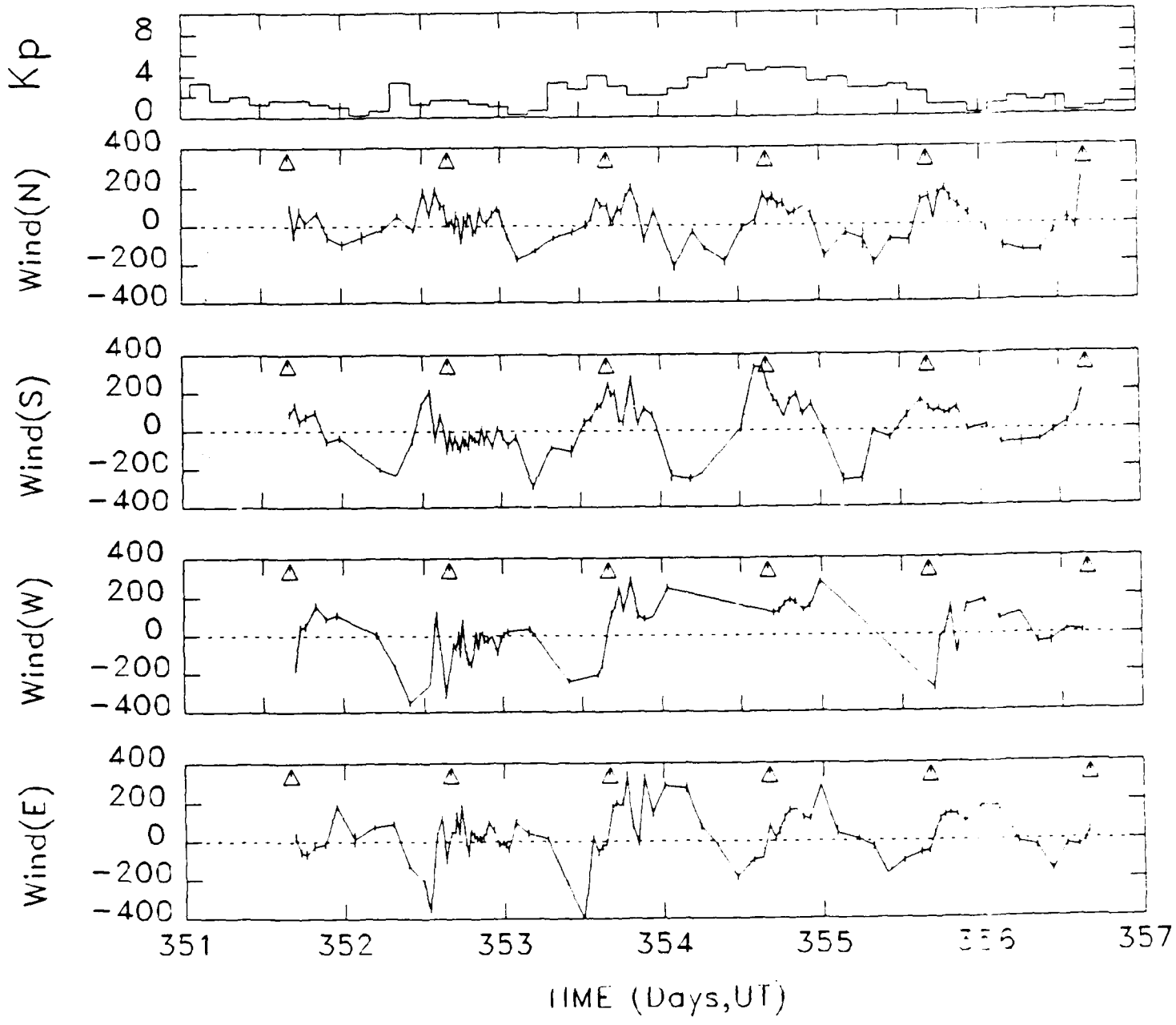
Kp
8
4
0
Wind(N)
400
200
0
-200
-400
Wind(S)
Wind(W)
Wind(E)
351
352
353
354
355
356
357
TIME (Days,UT)

Fig. 3

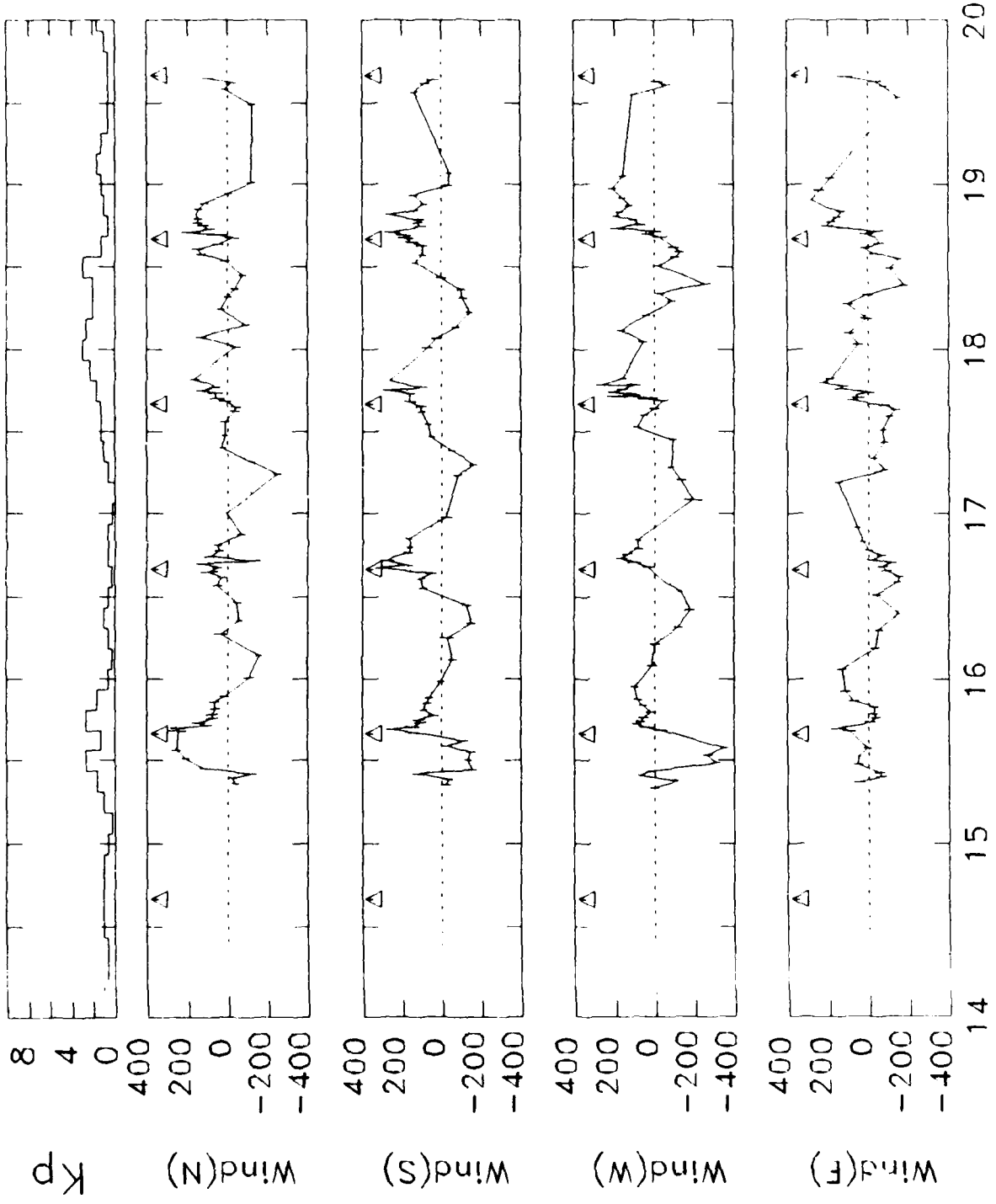
Kp
Wind(N)
Wind(S)
Wind(W)
Wind(E)
8
4
0
400
200
0
-200
-400
14
15
16
17
18
19
20
IIMt (Days,UI)

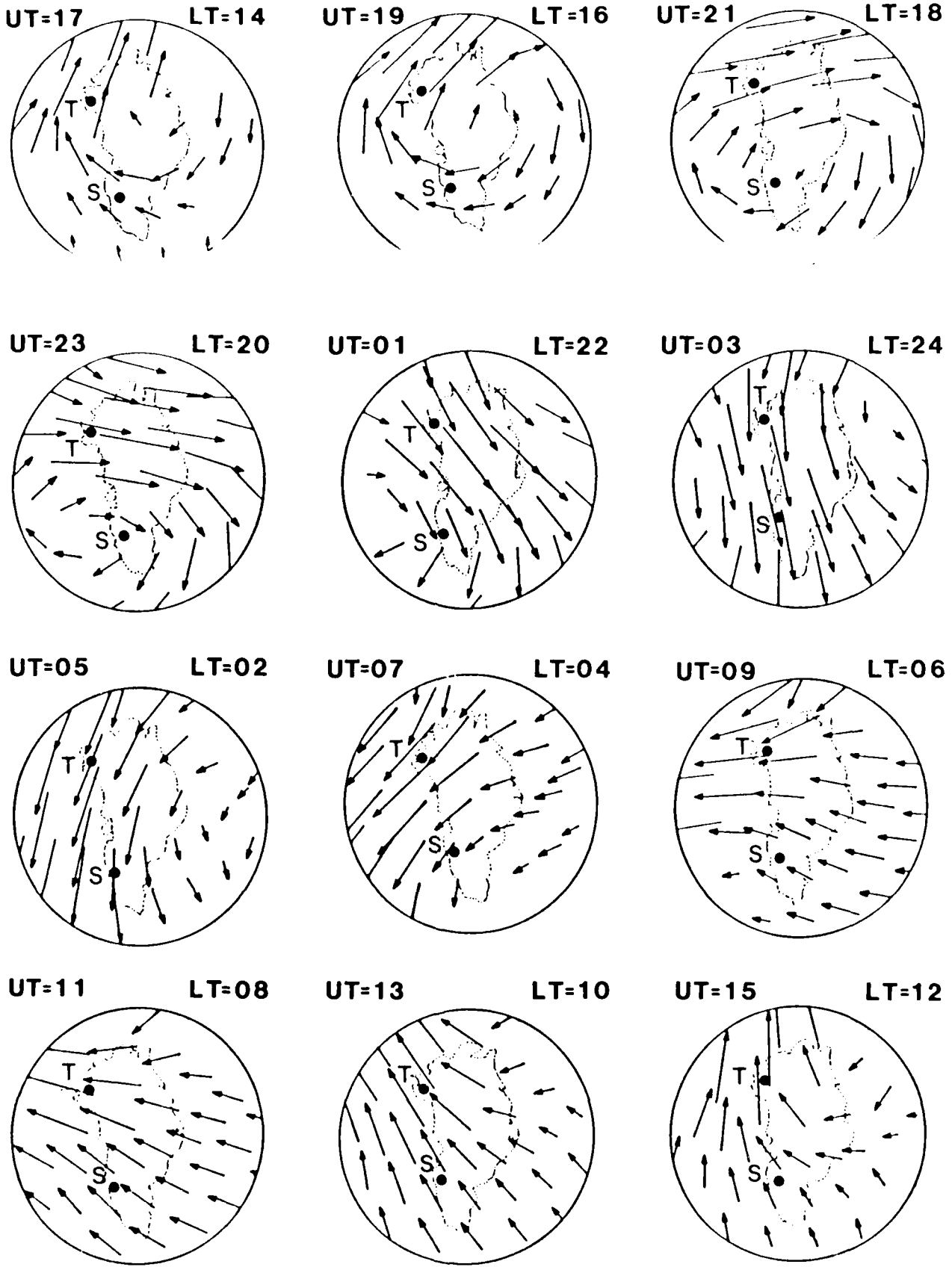
UT=17
LT=14
T
S
UT=19
LT=16
T
S
UT=21
LT=18
T
S
UT=23
LT=20
T
S
UT=01
LT=22
T
S
UT=03
LT=24
T
S
UT=05
LT=02
T
S
UT=07
LT=04
T
S
UT=09
LT=06
T
S
UT=11
LT=08
T
S
UT=13
LT=10
T
S
UT=15
LT=12
T
S

Fig. 5

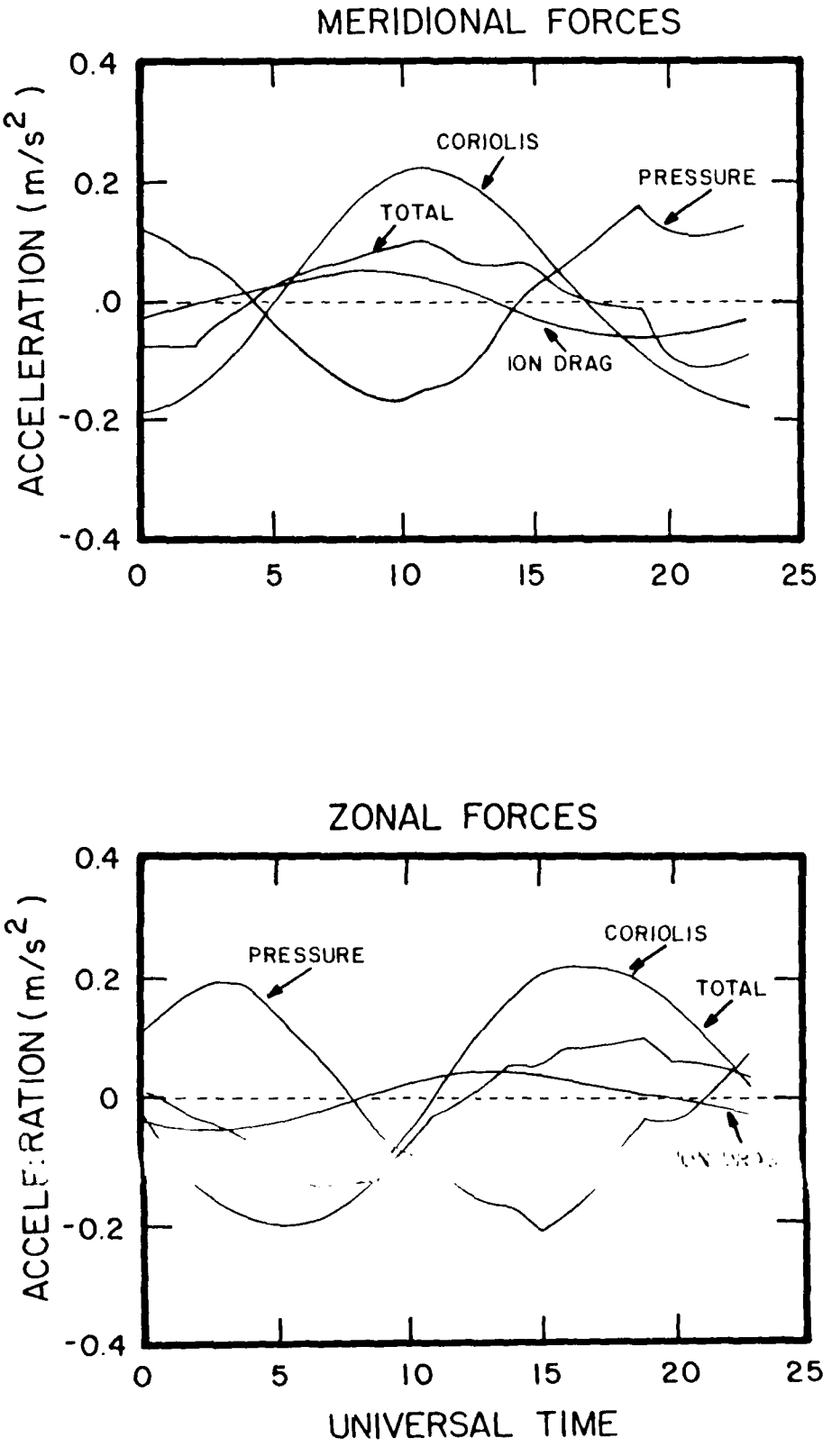
MERIDIONAL FORCES
ACCELERATION (m/s²)
0.4
0.2
.0
-0.2
-0.4
0
5
10
15
20
25
CORIOLIS
PRESSURE
TOTAL
ION DRAG
ZONAL FORCES
ACCELERATION (m/s²)
0.4
0.2
0
-0.2
-0.4
0
5
10
15
20
25
PRESSURE
CORIOLIS
TOTAL
UNIVERSAL TIME

Fig. 6

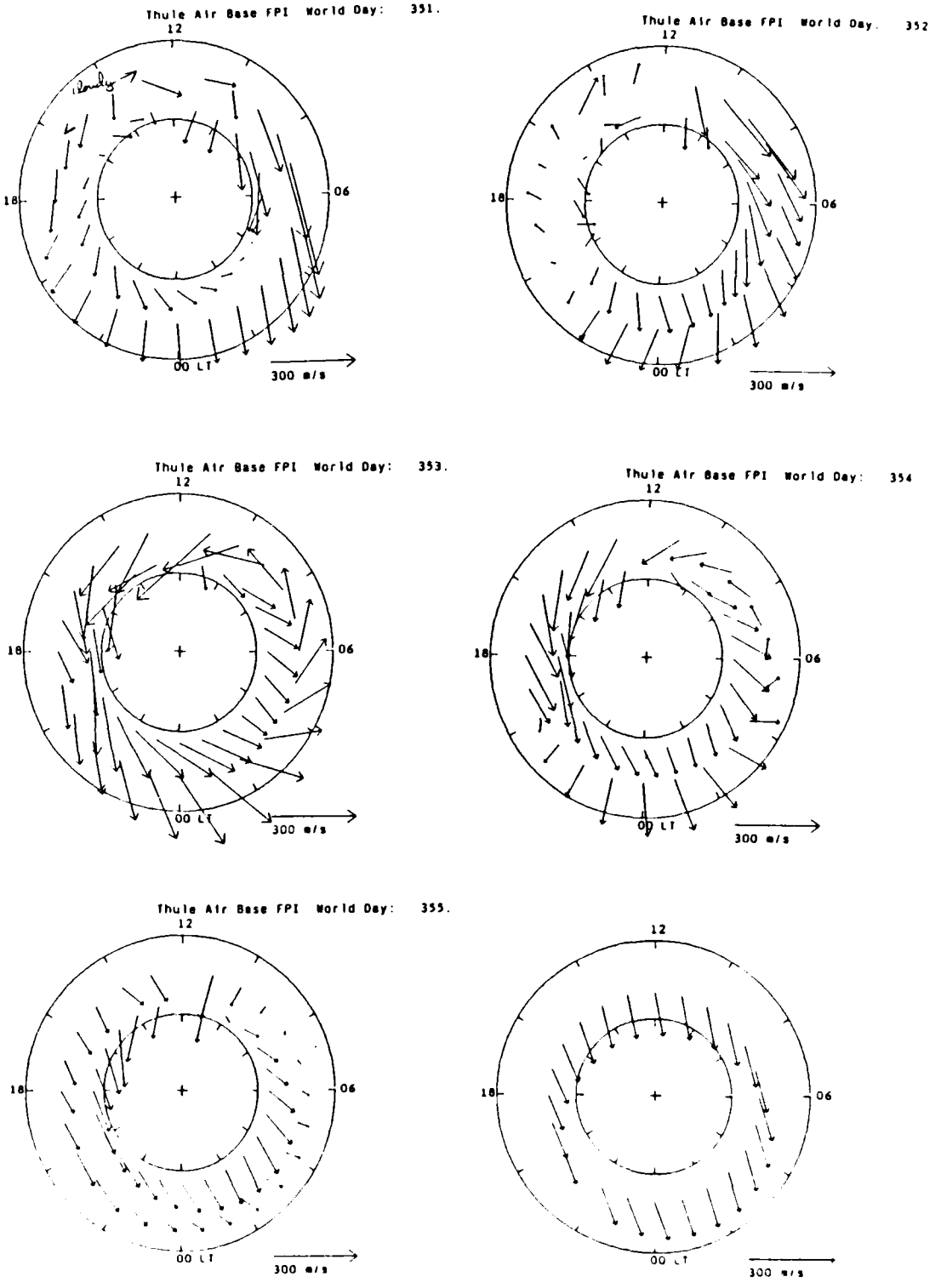
Thule Air Base FPI World Day: 351.
12
18
06
00 LT
300 m/s
Thule Air Base FPI World Day: 352
12
18
06
00 LT
300 m/s
Thule Air Base FPI World Day: 353.
12
18
06
00 LT
300 m/s
Thule Air Base FPI World Day: 354
12
18
06
00 LT
300 m/s
Thule Air Base FPI World Day: 355.
12
18
06
00 LT
300 m/s
12
18
06
00 LT
300 m/s

Fig. 7

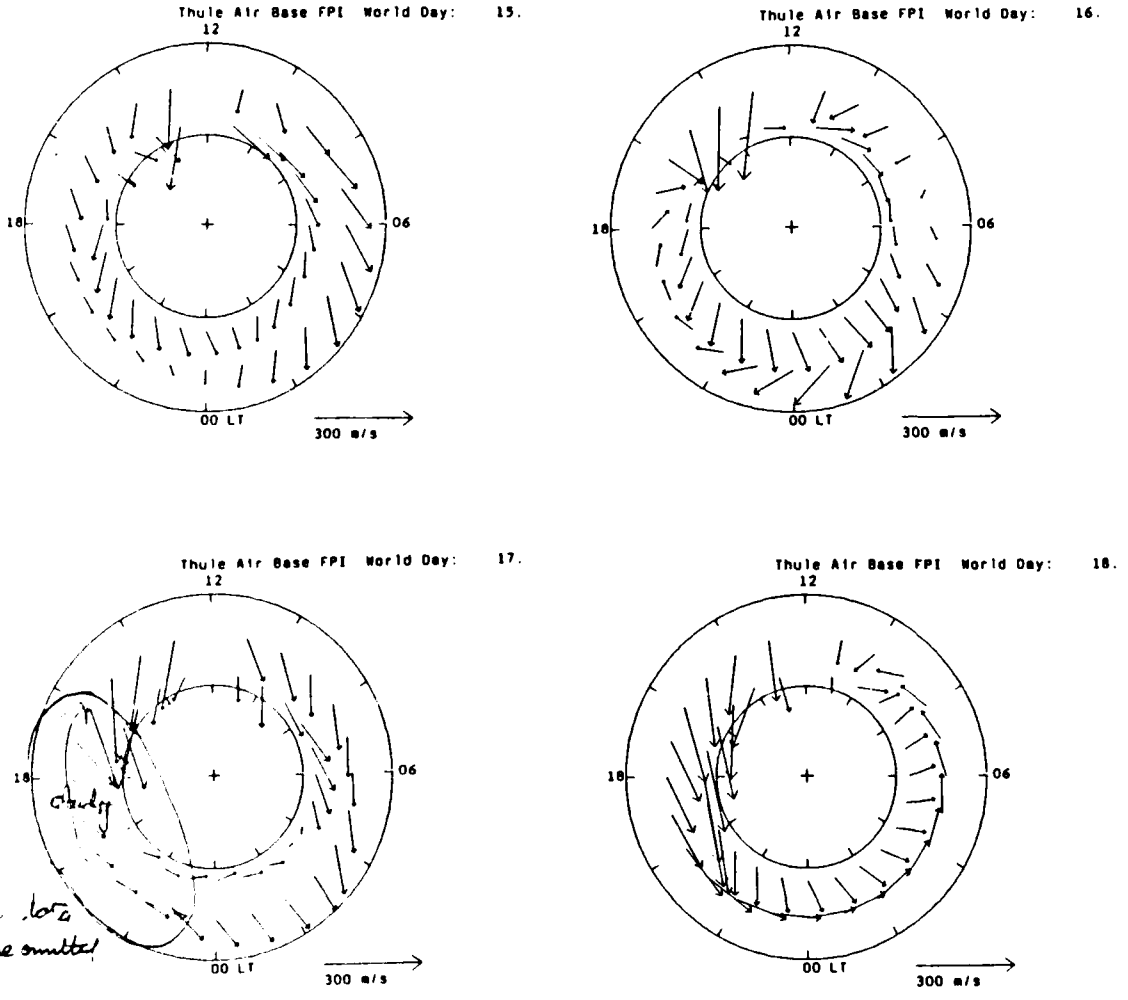
Thule Air Base FPI World Day: 15.
12
18
06
00 LT
300 m/s
Thule Air Base FPI World Day: 16.
12
18
06
00 LT
300 m/s
Thule Air Base FPI World Day: 17.
12
18
06
00 LT
300 m/s
Thule Air Base FPI World Day: 18.
12
18
06
00 LT
300 m/s

Fig. 8

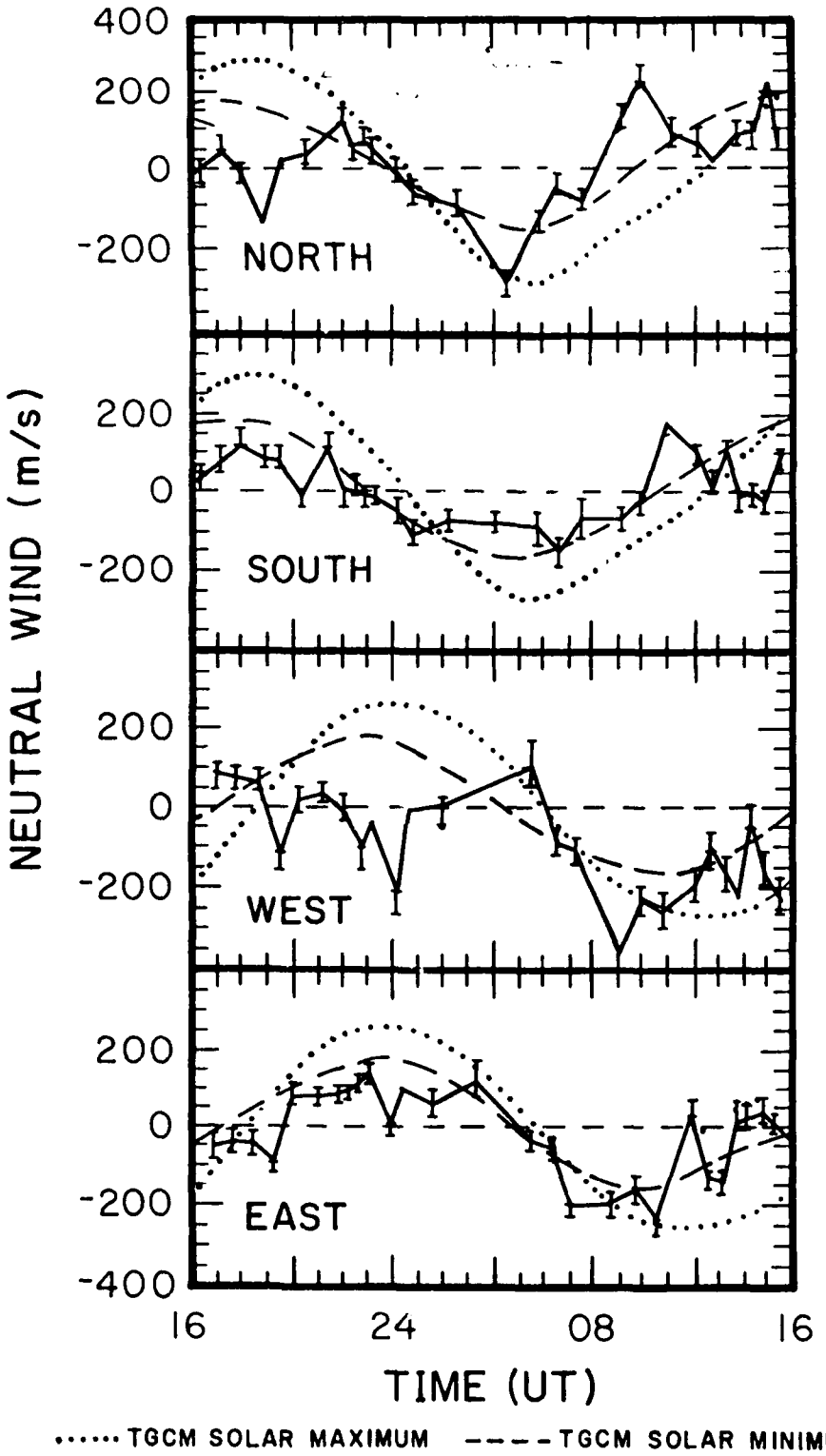
400
200
0
-200
NORTH
200
0
-200
SOUTH
200
0
-200
WEST
200
0
-200
-400
EAST
NEUTRAL WIND (m/s)
16
24
08
16
TIME (UT)
TGCM SOLAR MAXIMUM
TGCM SOLAR MINIMUM

Fig. 9

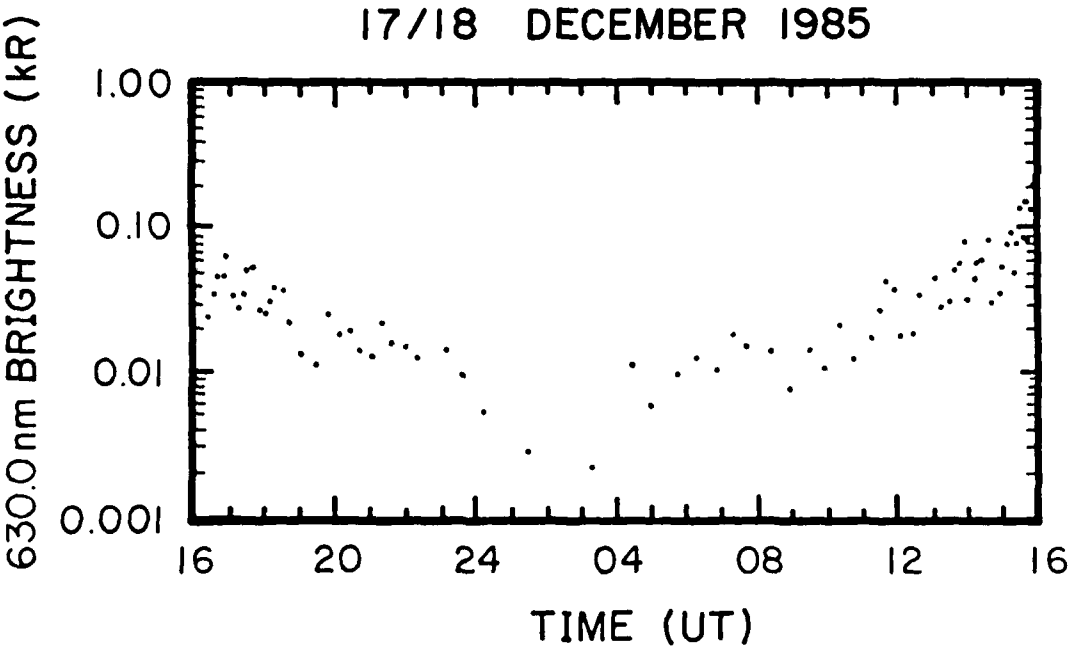
17/18 DECEMBER 1985
630.0nm BRIGHTNESS (kR)
1.00
0.10
0.01
0.001
16
20
24
04
08
12
16
TIME (UT)

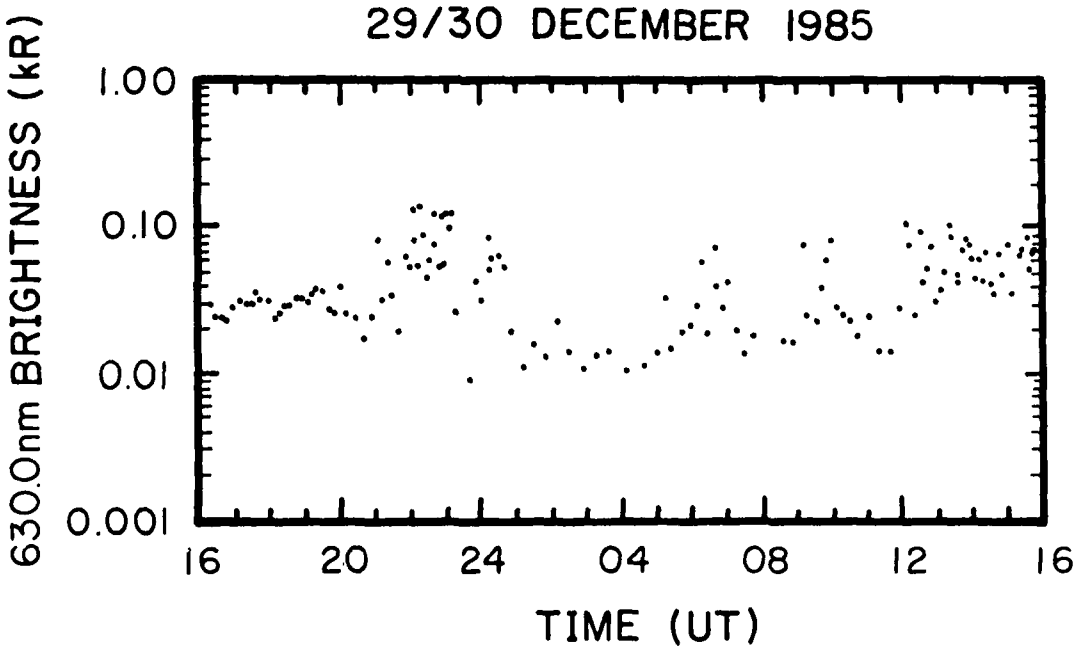
29/30 DECEMBER 1985
630.0nm BRIGHTNESS (kR)
1.00
0.10
0.01
0.001
16
20
24
04
08
12
16
TIME (UT)

Fig. 10

END

Feb.

1988

DTIC